MEASUREMENT OF THE THICKNESS AND REFRACTIVE INDEX OF EVAPORATED DIELECTRIC FILMS

MEASUREMENT OF THE THICKNESS AND REFRACTIVE INDEX OF EVAPORATED DIELECTRIC FILMS

PROEFSCHRIFT

TER VERKRIJGING VAN DE GRAAD VAN DOCTOR IN DE TECHNISCHE WETENSCHAPPEN AAN DE TECHNISCHE HOGESCHOOL DELFT, OP GEZAG VAN DE RECTOR MAGNIFICUS DR. IR. C. J. D. M. VERHAGEN, HOOGLERAAR IN DE AFDELING DER TECHNISCHE NATUURKUNDE, VOOR EEN COMMISSIE UIT DE SENAAT TE VERDEDIGEN OP WOENSDAG 8 MEI 1968 TE 16 UUR

DOOR

WILHELMUS VAN VONNO

natuurkundig ingenieur

geboren te Hilversum

UITGEVERIJ WALTMAN — DELFT

DIT PROEFSCHRIFT IS GOEDGEKEURD DOOR DE PROMOTOR

PROF. DR. H. DE LANG.

Aan Tineke

Aan mijn ouders

CONTENTS

SUMMARY

The purpose of this work was to obtain quantitative data of aging effects in the optical properties of dielectric thin films. The characteristic optical parameters of a thin film are the optical thickness, the refractive index and the possible absorption of the film. In order to study the changes in the optical parameters, it is necessary to be able to carry out measurements on the film in vacuo immediately after its manufacture by evaporation. In the introduction a brief review is given of the methods available for the measurement of optical parameters of thin films. It appeared desirable to use rather sensitive methods, whereby the parameters desired are immediately available; moreover the methods to be chosen had to be suitable for use in vacuo. There are some interferometric methods like that of VAN HEEL and WALTHER and the three slits method of ZERNIKE that are rather simple to use. Such interferometric methods, with the specimen in transmission have in common that a phase retardation is measured from which, in most cases, it is simple to deduce the optical parameter $(n-1)d$. In order to keep the error in the measurement of the optical path difference within $\lambda/1000$ it was necessary to introduce a photoelectric setting criterion instead of a visual one. A further advantage of a photoelectric interferometer is that it can operate with a very low luminous flux. This offered the possibility to use a very simple interferometer, based on YOUNG's double slit experiment.

This interferometer is described in chapter II. The phase retardation of a thin film is determined by measuring the shift of the interference fringes, which occurs if the film is inserted in one of the two light beams. First a setup is described in which a visual setting criterion due to FRANÇON and SOULIÉ is used. In fact this is a photometric criterion adjusting at a minimum of the diffraction pattern making use of the symmetry of this pattern. Next three photoelectric interferometers are described: (a) a setup using transmitted light, (b) a setup using reflected light and (c) a setup for measurements in vacuo. In order to obtain a suitable photoelectric criterion the position of the fringe pattern is modulated time harmonically. The modulation is achieved by an oblique plane-parallel glass plate rotating about the optical axis of the interferometer. The fringe position is determined with the aid of a slit and a photomultiplier. The photoelectric signal is a cosine function, the argument of which contains three contributions: (i) the position of the slit, (ii) the phase difference of the interfering beams and (iii) a time harmonic modulation term. In the fourier spectrum the odd harmonics, in particular the first harmonic, vanish if the first two contributions approach zero. The criterion of adjustment at this situation is the visual observation of the symmetrical waveform on an oscilloscope. The theory of this interferometer is

considered taking into account the degree of coherence, the finite slitwidth of the double slit and the intensity difference between the two interfering beams.

The phase retardation of a film can be put equal to $2\pi(n-1)d/\lambda$, if the multiple reflections and the absorption are negligibly small. In chapter III the validity of this approximation is discussed for the present high precision measurements.

For a direct measurement of the refractive index of a thin dielectric film we have chosen the ABELÈS method, because of its accuracy and simplicity. If a substrate is partly coated with a fully transparent film, then it can be shown that the reflectivity of the coated part of the substrate will be equal to that of the uncoated part, if the angle of incidence is equal to the Brewster angle of the film. This provides a very simple method for the measurement of the refractive index of fully transparent, homogeneous isotropic thin films. In chapter IV the sensitivity of this method is discussed. A description is given of two setups. One for measurements in air and the other for measurements in vacuo. In the latter case special measures had to be taken in order to avoid angular adjustments in the vacuum chamber.

In chapter V some results of measurements are given concerning the changes in the optical parameters $(n-1)d$ and n of thin dielectric films in consequence of aging effects. We have restricted ourselves to dielectric films commonly used in optics. The films were manufactured by evaporation of the material from a tantalum or tungsten boat in a vacuum chamber. Measurements were carried out while varying the deposition rate and the pressure in the vacuum chamber. The data obtained clearly show that the aging effects for the various film materials differ considerably. The aging process takes place in two steps: (i) an abrupt change immediately after the admittance of air, (ii) a more gradual change in the course of several days.

CHAPTER I

INTRODUCTION

In 1892 H. D. TAYLOR discovered a decrease in reflection associated with the tarnish which develops on flint glass surfaces. After this various chemical treatments were used to produce this 'tarnish' to decrease the intensity reflected on lens surfaces. Though evaporated metal films have been known since 1912 it was not before 1936 that J. STRONG wrote about an evaporated dielectric film to decrease the intensity reflected, an anti-reflection coating. Since then there has been a rapid development in new applications of evaporated dielectric films in optics, on which ever-increasing demands are being made. These applications are: multilayer anti-reflection coatings, mirrors for lasers, interference filters, beam splitters and protective layers for front surface mirrors. In the past twenty years much work has been done on the technology of the manufacture of thin films, the structure, the measurement of the optical constants, mechanical stress and adhesion.

To manufacture optical coatings with characteristic optical parameters, it will be necessary to control the evaporation in any event. This evaporation, however, takes place in vacuo just like the control. After the manufacture the coatings will be used in air in most cases. A difficulty is presented by the fact that the air will influence the optical properties of the films. From a scientific point of view this phenomenon is interesting, but practically seen it is necessary to have quantitative data of this effect on the optical thickness, the refractive index and the possible absorption of the film. Then the operator could correct these changes by producing a coating in vacuo with a predetermined deviation from the values desired. In order to study these changes in the optical constants, it is necessary to compare their values as measured in vacuo with those measured in air. A brief review will be given of the methods available for the measuring of optical constants of thin films.

A. Measurement of optical constants of thin films in air and vacuo

There are several methods available for the determination of the optical constants of thin films. The methods may be classified as being optical and non-optical.

1. *Optical methods*

a. *Colours of thin films*

The well-known phenomenon of 'colours of thin layers', discovered by BOYLE and HOOKE, was studied intensively for the first time by NEWTON ($\sim$ 1670). YOUNG explained this phenomenon as an interference effect for the first time in 1802. The

phenomenon occurs on thin transparent layers as 'interference of equal thickness'. After FIZEAU this effect has been employed extensively for thickness determinations. A review of the various methods which utilize interference colours for determining film thicknesses has been published by METHFESSEL [1]. For thickness measurements during deposition the colour of a test piece located close to the sample is viewed in reflection. According as the thickness of the film increases, the same colour may appear several times. If the film is being observed during deposition, the sequence of colours is noted and the deposition interrupted upon attaining the proper spectral order and colour. Several tables have been published for the corresponding thickness [2]. With this method the film thickness can be kept within 10%. In modern practice this method is almost completely abandoned.

b. *Measurement of the reflected or transmitted intensity*

A more precise and objective measurement of film thickness can be performed by measuring the total intensity of either the transmitted or reflected beam with the aid of an electric photodetector instead of the human eye, using light in a suitable spectral range. The intensity transmitted, i.e. *transmissivity*, of non-absorbing material (refractive index n) on a dielectric substrate (refractive index n_s) is a periodical function of the optical thickness (nd) of the film. The transmissivity has maxima and minima for optical thicknesses equal respectively to odd and even multiples of a quarter of a wave-length, if $n < n_s$. The position of the maxima and minima is reversed for $n > n_s$. Because there are no losses the transmissivity and *reflectivity* (reflected intensity) are complementary. In most cases of dielectric films in optics, the optical thickness of the individual layers should be multiples of a quarter of a wave-length ($\lambda/4$).

DUFOUR [3, 4] was probably the first one who used this method. FRÉMONT [5] was probably the first one who chopped the light beam employed for thickness measurement and introduced a colour filter to vary the wave-length and the thickness of the film for the $\lambda/4$ condition. The adjustment at minima or maxima is greatly facilitated by feeding the signal into a recorder [6]. While viewing the recorder trace, an 'integration by eye' over the portion of the trace proceeding the extremum is performed, and its location can be detected much more accurately than is possible from a galvanometer. With this refinement the accuracy in film thickness can be kept within 2%. Thus determination of optical thicknesses, that are multiples of $\lambda/4$, is easy with a method that detects maxima and/or minima of the reflectivity or transmissivity during film deposition. However, the adjustment itself at maxima and minima is rather poor. A much better accuracy is achieved by GIACOMO and JACQUINOT [7] by using modulation of the wave-length by vibrating the mirror of the monochromator.

For strongly absorbing films the transmissivity will show a strong exponential decrease according as the thickness increases. This decrease provides measurement of film thickness. In these cases the method can be used only for very small thicknesses.

For the measurement of refractive indices of fully transparent films ABELÈS has devised a very simple method [8, 9] (fig. 1). A collimated beam of light polarized in the plane of incidence is incident on a surface partly covered by the film under in-

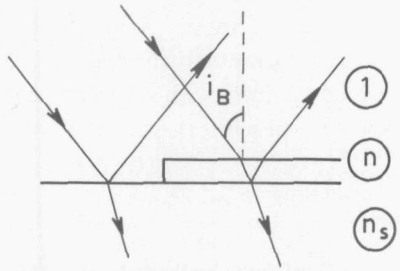

Fig. 1. The ABELÈS method for measurement of the refractive index of a thin film. If the reflectivities of both parts of the specimen are equal to each other, then $\tan i_B = n$.

vestigation. The angle of incidence i_B for which the reflectivity of film and substrate are equal is determined. It can easily be shown that the refractive index n of the film is given by:

$$n = \tan i_B \tag{1}$$

if the light is incident in air. Note that this relation does contain neither the thickness of the film nor the optical constants of the substrate. The *sensitivity* of the method does depend, however, on these parameters. For the case of a film, provided that the index of the film lies within about 0.3 of that of the transparent substrate, a measurement within 0.002 is possible if the optical thickness of the film is in the region of odd multiples of a quarter of a wave-length. Varying the wave-length the dispersion effects can be measured. Since the condition of equal reflectivity is completely independent of the refractive index of the substrate, this method can be used for films on absorbing surfaces.

The great advantage of the ABELÈS method lies in its simplicity. The disadvantage, i.e. that the optical thickness of the film to be measured has to be in the region of odd multiples of a quarter of a wave-length, is not very serious in practice.

c. *Ellipsometry*

This method makes use of the anisotropy of oblique reflection (DRUDE [10]). This anisotropy provides full information of the optical parameters of the reflector. This method is very effective. However, a somewhat tedious mathematical procedure is necessary to computate the complex refractive index and the thickness from this anisotropy, which makes the method less suitable for monitoring in vacuo. HERMANSEN has described a method on this principle for measurements in vacuo [11].

d. *Interferometric methods*

Polarization interferometry. In all interferometers of this kind the incident beam is devided into two polarized beams. One of the simplest arrangements is the eyepiece devised by FRANÇON [12]. A plane polarized (fig. 2) collimated beam emerges from the specimen with the wave-front deformed. With the aid of the Savart plate the wave-front is split up into the two mutually perpendicularly polarized component wave-fronts which are displaced laterally with respect to each other. Viewed through the analyser the field of view will then in general show three areas of different inten-

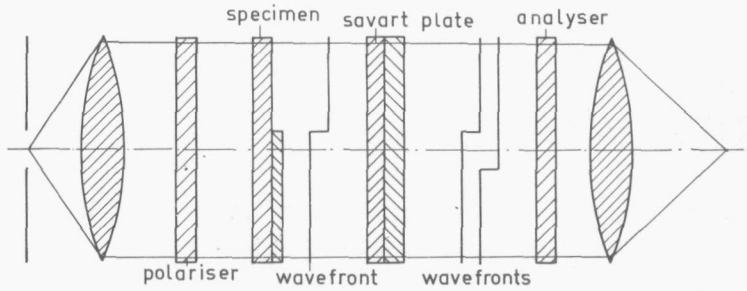

Fig. 2. Principle of a filmthickness measurement using the FRANÇON eyepiece by VAN HEEL.

sities. These differences form a measure for the phase thickness of the film. Various experimental arrangements are discussed by VAN HEEL and WALTHER [13]. An accuracy in phase thickness of $\lambda/200$ can be attained for transparent films on transparent substrates. Furthermore, if the transmissivity of the film is also measured, both the thickness and refractive index can be determined. Since normal incidence is used and since the specimen does not need to be metallized, the method is suitable for rapid measurements in vacuo.

Instead of a Savart plate a Wollaston prism is used in the shearing interference system devised by DYSON [14]. In this case the film under examination has to be metallized. Ligth from a slit is projected via the Wollaston prism, on to the metallized,

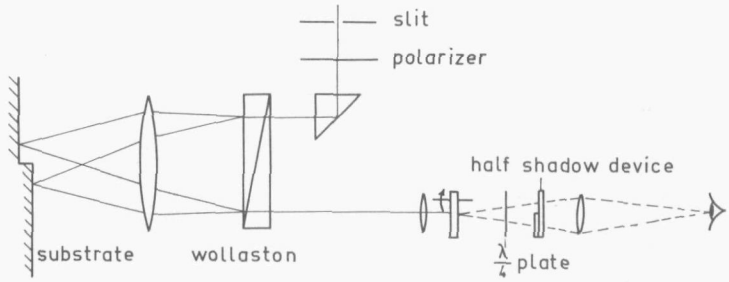

Fig. 3. DYSON's shearing interference system for thickness determination.

partly coated, substrate, producing two images at the surface which are perpendicularly polarized (fig. 3). On passing through the Wollaston prism for the second time, the images are combined and the final image is examined through a polarizer and a half-shadow system. DYSON has reported that the geometrical thickness can be measured within $\lambda/5000$. The arrangement can not easily be used in vacuo for monitoring, because of the metallizing.

Non-polarizing interferometry. One of the simplest methods for measuring film thickness is that using multiple beam interference fringes [TOLANSKY, 15]. The partly coated substrate is metallized. The interference takes place between this metallized surface and a heavily metallized reference flat. Taking the right precautions the fringes are extremely fine and an accuracy of $\lambda/500$ in film thickness can be obtained. This method has been used in vacuo by GREENLAND and BILLINGTON [16]. An analogous method was used by SCHULZ [17]. Here the metallized specimen act as one mirror of the Fabry-Pérot interferometer.

In principle the fringe displacement, caused by a film, can be measured by any type of interferometer. The ordinary Michelson interferometer for instance was used by FOCHS [18] and R. PRAT and M. L. ROBLIN [19]. These methods have not been used in vacuo. ZERNIKE used an arrangement with three slits [20] to measure phase strips for microscopy. (In fact this work was a rediscovery of the work of VÄISÄLÄ [21].) The diffraction pattern of three equidistant slits may be considered as being formed by the fringes of equal intensity caused by the outer slits, together with the coherent background from the middle slit, which alternately reinforces and suppresses the peak intensity of these fringes. This effect disappears when the focus of the observing telescope is changed so as to cause a geometric path difference of an odd multiple of a quarter of a wave-length between the middle and outer beams resulting in two accurate setting criteria, for which all the fringes are of equal brightness. A phase

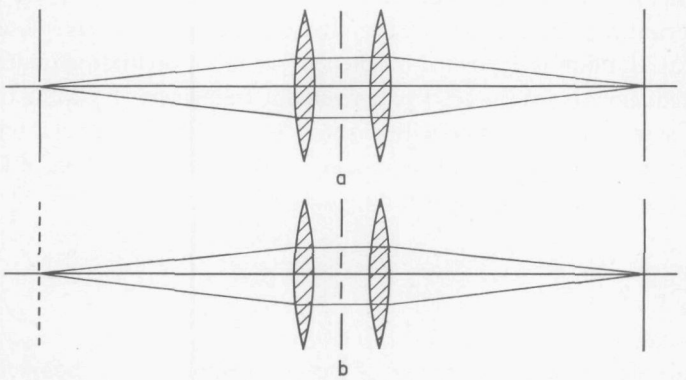

Fig. 4. The three slits interferometer by: a. ZERNIKE; b. LOHMANN.

strip in front of the middle slit gives an outward or inward shift of these setting criteria, which is a measure for its path difference with an accuracy of $\lambda/200$. VAN HEEL [22] used this method to measure path differences of magnesium fluoride films. A. LOHMANN [23] improved this method by using three coherent maxima generated by an optical grating (fig. 4). The period of this grating coincides with the period of the diffraction fringes. The advantage is that more light is available, which increases the accuracy ($\lambda/500$).

The three slits method is not reported to have been used in vacuo.

2. *Non-optical methods*

a. *Electrical methods*

For metallic films, the measurement of film resistance can provide information about the thickness of the film. However, the relation between resistance and thickness of the film is rather uncertain, especially at low film-thickness, due to island formation of the film. Therefore resistance measurements can give a reliable indication of film thickness, if the film is fabricated under well-defined conditions to obtain comparable values from run to run. Then the thickness can be measured within 4%.

Another method to determine film thickness makes use of the measurement of the change in capacitance of a capacitor, if a dielectric film is deposited on it [24]. This method can only be applied to dielectric films. A new capacitor has to be used for every deposition. It is also possible in this case to measure the thickness within 4%.

b. *Determination of film thickness by measuring its mass*

In vacuo it is possible to measure the mass of a film by a very sensitive torsion-microbalance. See for instance [25]. An accuracy of 10^{-8} gram, corresponding to a few Ångströms in film thickness, has been achieved. As the arrangement is a vulnerable one, it is a method suitable for laboratory work rather than for routine work.

A very elegant method for mass determination of thin films makes use of a crystal oscillator [26]. If a film is deposited on the surface of an oscillating quartz crystal the change in frequency is measured. For a resonant frequency of 5 Mc/s the frequency change can be measured easily to within about 1 c/s. If the test crystal has a mass M_0 of a resonant frequency ν_0, than the frequency change $\Delta\nu$ for a film of thickness Δd, surface F and specific mass ϱ is given by:

$$\frac{\Delta\nu}{\nu_0} = \varrho\frac{\Delta d \cdot F}{M_0} \tag{2}$$

For a typical case a frequency change of 1 c/s corresponds to a change in film thickness of 3 Å for aluminium [27].

B. Choice of a suitable method

We had a vacuum chamber (500 mm ⌀ and 650 mm high) at our disposal (Balzers BA 500). This vacuum chamber was equiped with a modulated beam photometer (fig. 5), a setup for measuring the reflectivity and transmissivity, according to I.A.1.b. A light source is imaged at the sample by two lenses. The film on the sample can be measured during deposition either in transmission by the photocell on top of the bell jar or in reflection by the photocell below. Chopping of the light results in an AC-signal from either photocell. A narrow band amplifier tuned to the chopping

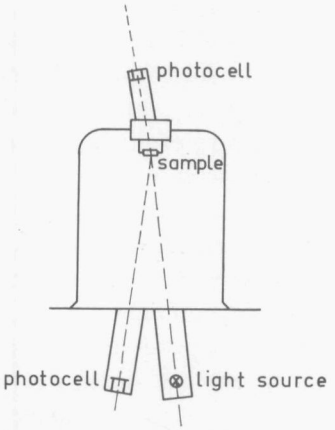

Fig. 5. Modulated beam photometer in vacuum chamber. An arrangement to measure the reflectivity and/or transmissivity as a function of the optical thickness of the film.

frequency, rejects signals caused by steady or slowly varying background illumination at lower frequencies, or filaments, lamps, etc. at higher frequencies. The amplified signal is fed into a recorder. The accuracy of this photometer, which is about 2%, is sufficient to make anti-reflection coatings, dichroic mirrors and mirrors for lasers, but it is unsufficient for the fabrication of narrow pass band interference filters with an accurately prescribed location of the transmission peak.

Further, a recording spectrophotometer (Spectronic 505, Bausch and Lomb) was available with which continuous graphs of transmissivity versus wave-length can be obtained in the range 3500 to 7500 Å. The absolute uncertainty was about 0.5%.

The transmissivity and reflectivity by oblique incidence were measured by an available setup for angles of incidence between 10° and 80°. The absolute uncertainty was about 0.5%.

The properties of a film that play a role in the possibilities for optical use of that film are the optical thickness *nd*, the refractive index *n* and the absorption. In practical use it is necessary to know the behaviour of these properties as a function of time.

In order to study such aging effects, it is desirable to have a rather sensitive method,

whereby the optical constants are immediately available. The modulated beam photometer, described above, is not very suitable for this purpose, because of its sensitivity and because of the fact that it does not give the optical properties directly. Further, the phase retardation cannot be determined. We prefer not to use the polarimetric methods because of the computations they necessitate. The method of DYSON is sensitive enough, but it can only be used for metallized films. Besides, only the geometrical thickness can be measured. This also holds good for the method of TOLANSKY. A crystal oscillator and a micro-balance are sensitive enough, but they also only give information about the geometrical thickness.

Among the interferometric methods, that of VAN HEEL and WALTHER and the three slits method of ZERNIKE, VAN HEEL and LOHMANN are rather simple to use. Moreover, all interferometric methods, with the specimen in transmission, have in common that the phase retardation is measured from which in most cases it is rather simple to deduce $(n-1)d$. However, the accuracy of these methods, when used visually, is not quite sufficient to measure the effect with sufficient accuracy.

Therefore we needed a method suitable for measurements in vacuo of the path difference caused by a thin film with an accuracy of about $\lambda/1000$. Besides, it would be very convenient if the optical thickness could be determined from this measurement in a simple way. The only way to obtain this accuracy is by using photoelectric criteria instead of visual ones. This makes it possible to use a very simple interferometer, based on YOUNG's double slit experiment, which does not exclude the use of other methods. The interferometer will be described in chapter II and III.

For a direct measurement of a refractive index we choose the ABELÈS method, because of its simplicity. A detailed description will be given in chapter IV.

In chapter V the results of measurements on several materials of practical interest will be given.

CHAPTER II

PHASE MEASUREMENTS WITH YOUNG'S DOUBLE SLIT ARRANGEMENT

THOMAS YOUNG was the first to give an adequate explanation of the interference phenomenon in particular for the case of coherent lighted slits. He wrote in 1807 [28]: . . . the simplest case appears to be, when a beam of homogeneous light falls on a screen in which are two very small holes or slits, which may be considered as centres of divergence, from whence the light is diffracted in every direction. In this case, when the two newly formed beams are received on a surface so as to intercept them, their light is divided by dark stripes into portions nearly equal, but becoming wider as the surface is more remote from the apertures at all distances, and also wider in the same proportions as the apertures are closer to each other . . .

In fact this arrangement embodies a very simple form of a two beam interferometer. In this case the two beams are hardly laterally separated, which makes the arrangement insensitive to disturbances. This is very convenient for our purpose, the use of the arrangement in a vacuum chamber. A disadvantage of the double slit method is the fact that the luminance is rather poor.

FRESNEL and ARAGO (1816) were the first to determine the phase retardation of a phase object by measuring the shift of the interference fringes, which occurs if the phase object is placed before one of the two slits. If the measurement is done visually, the accuracy with which the shift can be determined is too low, even if very elegant setting criteria, like the one of FRANÇON and SOULIÉ [29], are used. Besides the use of a visual setting criterion is very tiresome. As such criteria involve a comparison of two luminances at the same time, the way to solve the problem could be the use of two photoelectric detectors instead of the human eye. However, it is much easier to use only one detector in order to compare intensities one after the other, thus separated in time. We have done this by harmonic modulation of the interference fringes. Others, who have been using modulation for adjustments are, for instance, K. M. BAIRD [30], R. D. HUNTOON, A. WEISS and W. SMITH [31].

A. Principle of the double slit interferometer

A collimated beam of monochromatic light (wave-length λ) is transmitted by two parallel slits (fig. 6). A diffraction pattern is formed in the focal plane of a lens. This pattern will have a sinusoidal intensity distribution. If the collimation is ideal and the bandwidth is zero, further assuming that the width of the two slits is a small fraction of the distance h of the two slits, then the intensity I in the focal plane will be

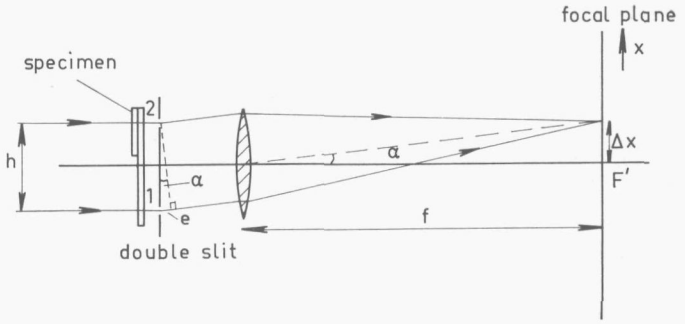

Fig. 6. Principle of phase retardation measurements with YOUNG's double slit arrangement.

$$I = I_0\left[1+\cos\left(\frac{2\pi h \sin\alpha}{\lambda}\right)\right] \tag{3}$$

In practice $h \gg \lambda$, so that only small α values need to be taken into consideration. Then it is easy to see from (3) that

$$I = I_0\left[1+\cos\left(\frac{2\pi h}{\lambda f}x\right)\right] \tag{4}$$

where f is the focal length of the lens.

A partly coated plane-parallel glass substrate is placed in front of the two slits. The film is positioned in such a way that it covers only one of the two slits. The light passes through the substrate perpendicularly. Now there will be a phase difference between the light from slit 1 and 2. This will cause a shift Δx of the diffraction pattern perpendicular to the optical axis. The intensity I will be

$$I = I_0\left[1+\cos\left(\frac{2\pi h}{\lambda f}x - \frac{2\pi e}{\lambda}\right)\right] \tag{5}$$

where e is the optical path difference caused by the film. From (5) and fig. 6 can be seen, that e will be

$$e = \frac{h\Delta x}{f} \tag{6}$$

For the successive maxima of the diffraction pattern the optical path difference changes by λ. It is easy to see (3), that the period p of the maxima respectively minima is:

$$p = \frac{f\lambda}{h} \tag{7}$$

(6) and (7) give then

$$e = \frac{\Delta x}{p}\lambda \tag{8}$$

Ignoring the multiple reflections and absorption in the film, the optical path difference e between the two wave-fronts is too

$$e = (n-1)d \tag{9}$$

where n is the refractive index and d the geometrical thickness of the film. So

$$\underline{(n-1)d = \frac{\Delta x}{p}\lambda} \tag{10}$$

Thus measurement of the shift Δx and the fringe distance p immediately determines the phase retardation of the film, if λ is known. However, the fringe distance p is, under the above-mentioned approximations, independent of the optical properties of the film. Thus p can be considered as a constant of the experimental setup, that has to be measured once. Thus for different films the shift Δx is the only quantity, that has to be determined.

B. A purely visual photometric method for fringe location

For a long time the usual way for fringe location has been to use a reticle or another fiduciary mark. In general then the fringe can be located within $\lambda/50$. KENNEDY (1926) was the first to realize that the use of a half-shadow method, similar to the one used in polarimetry, improves the accuracy. He devised such a method for the Michelson interferometer, by raising one half of the surface of one of the mirrors a fraction of a wave-length above the other half [32]. This was done in such a way that the fringes are parallel to the dividing line. Under favourable conditions a setting error of $\lambda/500$ can be attained (see also BOTTEMA [33]).

A very good and simple half-shadow method is the one used by FRANÇON and SOULIÉ [29]. This method makes use of a slit placed parallel to the fringes. While the slit is observed with a microscope it is adjusted exactly at a minimum of the diffraction pattern (fig. 7a). If the slit is not adjusted exactly symmetrical with respect to this minimum the eye of the observer will see this immediately (fig. 7b). FRANÇON and SOULIÉ did the experiment with a Savart interferometer. They determined the setting

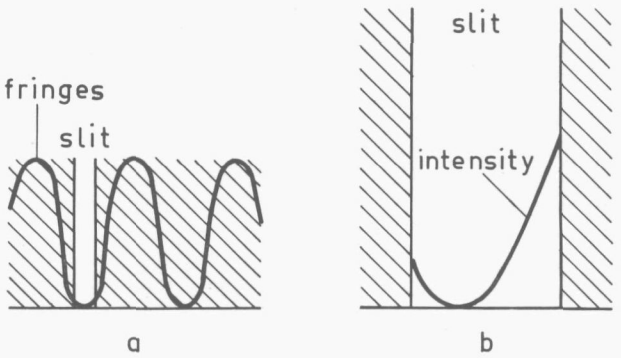

Fig. 7. a. The adjustment of the slit at a minimum of the diffraction pattern.
b. The observer sees immediately that the slit is not adjusted exactly at a minimum.

error as a function of the luminance and slit-width experimentally. Under the most favourable luminance conditions and an optimal slit-width, which appeared to be about 1/40 of the period of the fringes, they attained a setting error of $\lambda/4500$.

However, a simple calculation, similar to the one BOTTEMA [33] used for the method of KENNEDY, also gives an impression of the optimal slit-width. Up till now the visibility V of the fringes, defined by MICHELSON, was supposed to be unity. If this is not the case, due to stray light, false reflections, etc., the intensity distribution of the fringes can be written according to (5), (6) and (7) as

$$I = I_0\left[1+V\cos\frac{2\pi}{p}(x-\Delta x)\right] \tag{11}$$

Let the slit-width be b, then the intensity at the right side of the slit is

$$I_r = I_0\left[1+V\cos\frac{2\pi}{p}(x-\Delta x+\tfrac{1}{2}b)\right] \tag{12}$$

and at the left side

$$I_l = I_0\left[1+V\cos\frac{2\pi}{p}(x-\Delta x-\tfrac{1}{2}b)\right] \tag{13}$$

The contrast γ in the field of view is defined as

$$\gamma = \frac{I_r-I_l}{I_r+I_l} \tag{14}$$

As we adjust at a minimum, we are interested in the derivative γ' of γ to $x-\Delta x$ for $x-\Delta x = \pi$; from (12), (13) and (14) it follows that

$$\gamma'_\pi = \frac{V\frac{2\pi}{p}\sin\frac{b\pi}{p}}{1-V\cos\frac{b\pi}{p}} \tag{15}$$

The sensitivity of the adjustment is proportional to γ_π'. The maximum of γ_π' amounting to

$$\gamma'_\pi = \frac{\frac{2\pi}{p}V}{\sqrt{1-V^2}} \tag{16}$$

is obtained with an optimal slit-width determined by

$$\cos\left(\frac{b\pi}{p}\right) = V \tag{17}$$

For example $V = 0.95$ gives an optimal slit-width of about 1/30 of the period p and a setting error $\Delta x = p/4000$, assuming the threshold-value of the human eye to be a constant ($\Delta I/I = 0.01$) according to WEBER's law. In many practical cases, however, the luminance of the diffraction pattern is so low that WEBER's law is no longer valid and must be replaced by the law of WEBER-FECHNER:

$$\Delta I = C(I+I_c) \tag{18}$$

where I_c and C are subjective constants. This results in a larger optimal slit-width and a smaller sensitivity of the adjustment.

1. *Experimental setup*

A light source is imaged at an entrance slit by means of a condensor (fig. 8). The collimated beam passes through the partly coated substrate. The diffraction pattern of the double slit is formed in the focal plane of a lens. A slit in this plane (exit slit) is adjusted at a minimum of the diffraction pattern. This is observed by means of a microscope.

a. *The light source*

A mercury lamp was used to ensure a sufficiently monochromatic and bright light

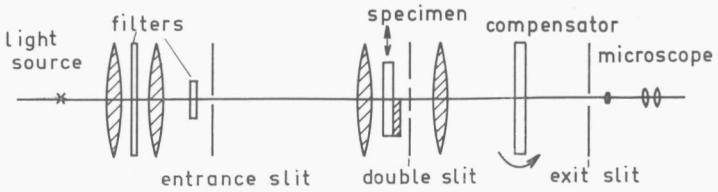

Fig. 8. Experimental setup.
The diffraction pattern is formed in the plane of the exit slit. This is observed by means of a microscope.

source. The 5461 Å emission line is the strongest one, so an interference filter was used for this wave-length. Besides a neodymium filter has to be used in order to suppress the yellow lines. A disadvantage of mercury lamps is that the intensity is irregular (the lamp flickers). This is annoying during the setting of the slit. We used the Philips HP 80, a mercury lamp which suffers least of all from this effect. The intensity of the diffraction pattern depends on the luminance of the light source, the degree of coherence desired and the ratio of the slit-width and the mutual distance of the double slit, but is independent of the absolute dimensions (see II. C. 2). So the absolute dimensions can be determined by practical considerations. For instance the mutual distance h of the double slit may not be too small in connection with the fact that the edge of the film on the substrate is not ideally sharp. As a result of experiments we obtained good results with: an entrance slit of 25 μ, a double slit of 350 μ width and a mutual distance h of 1234 μ, focal lengths of the lenses of 539 mm and a width of the exit slit of about one tenth of the period p of the fringe pattern.

The distance p is with these values 238.5 μ. So, to obtain an accuracy of $\lambda/1000$ in film thickness, the exit slit has to be adjusted in the plane of the diffraction pattern at 0.24 μ. This cannot easily be done in a mechanical way. Therefore this is done optically with the well-known tilted plane-parallel glass plate compensator.

b. *Translation with a plane-parallel glass plate*

If a parallel beam of light passes through a plane-parallel glass plate with an angle of incidence not equal to zero, the beam will undergo a lateral translation. To compute this translation $\Delta' x$ there are two equations:

$$\sin i = n' \sin i' \tag{19}$$

$$\sin(i - i') = \frac{\Delta' x}{d'} \cos i' \tag{20}$$

where i is the angle of incidence in air, i' the angle of refraction in the glass plate, n' the refractive index of the plate and d' the thickness of the plate (fig. 9). The expres-

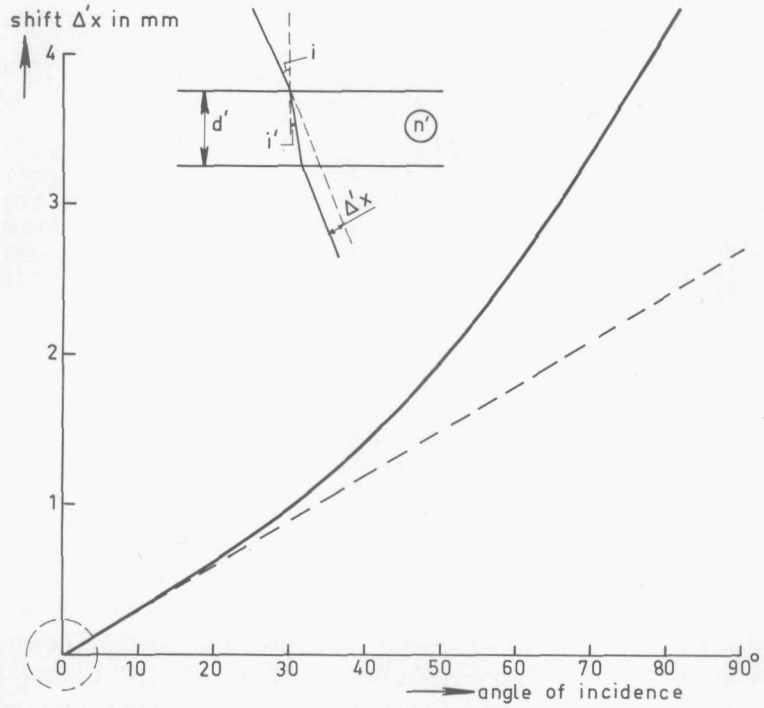

Fig. 9. Translation with a plane-parallel glass plate. The solid line corresponds with the exact expression of the shift as a function of the angle of incidence. The dotted line can be used for small angles of incidence. Table I shows the shift in the circled area. $d' = 5$ mm; $n' = 1.52$.

sions (19, 20) are exact, but it will often occur that the angle of incidence has small values, so that they can be simplified. Formula (19) and (20) become then:

$$\left.\begin{aligned} i &= n'i' \\ \Delta'x &= d'(i-i') \end{aligned}\right\} \tag{21}$$

This gives:

$$\Delta'x = d'i\frac{n'-1}{n'} \tag{22}$$

So for small angles of incidence i the translation $\Delta'x$ is proportional to i. That means that the shift Δx and the period of the fringes p can be determined by measuring the tilt of the plane-parallel glass plate to compensate the shift of the diffraction pattern. Then according to (10)

$$(n-1)d = \frac{i_{\Delta x}}{i_p}\lambda \tag{23}$$

TABLE I

Angle of incidence i	shift in μ $\Delta' x = \frac{d' \sin(i-i')}{\cos i'}$	shift in μ $\Delta' x = d' i \frac{n'-1}{n'}$	error in μ
1°	29.80	29.80	0.00
2°	59.61	59.61	0.00
3°	89.46	89.42	0.04
4°	119.40	119.22	0.18
5°	149.45	149.03	0.42
6°	179.55	178.83	0.72
7°	209.79	208.64	1.15
8°	240.20	238.44	1.76
9°	270.79	268.25	2.54
10°	301.47	298.05	3.42

Figure 9 and table I show the relations (20) and (22) for the case $d' = 5$ mm and $n' = 1.52$, as used in the setup. From the table it can be seen that the distance $p = 238.5$ μ is compensated by an angle of incidence of almost 8°. The error in the linear approximation is 1.76 μ, corresponding to a deficit of $\lambda/150$. For this measurement of i_p it is necessary to use the exact expression (20). The period p is compensated by i_p is about 8°, meaning that there will always be a minimum between an angle of incidence of −4° and +4° so that for the measurement of $i_{\Delta x}$ the error will never exceed 0.18 μ, corresponding to $\lambda/1350$. Thus in most cases $i_{\Delta x}$ can be substituted directly in (23) without correction.

The tilt of the plate was measured with a goniometer within 6″, which corresponds to an uncertainty in the thickness measurement of $\lambda/5000$.

c. *Substrate and film*

To avoid errors in the measured optical path difference, the substrate must have zero dioptric power, which means in practice the use of flat surfaces. A slight wedge-shape is not harmful.

In most cases the substrates were glass plates of $25 \times 25 \times 3$ mm, made of a good quality optical glass, Schott BK 7. Part of the substrate should be coated.

d. *Measuring procedure*

For the purpose of measuring the optical path difference, caused by the thin film, the substrate is placed as is shown in fig. 10a. A plane-parallel glass plate (compensator) is placed perpendicular to the optical axis of the setup (fig. 8). The exit slit is now adjusted provisionally at one of the first order minima of the diffraction pattern. After

this it is done precisely with the compensator. Now the substrate is placed as is given in fig. 10b. This gives a shift Δx of the diffraction pattern. The shift is compensated by rotating the glass plate over an angle $i_{\Delta x}$ till the first minimum that appears has been adjusted again. Now the substrate is placed as shown in figure 10c. In the ideal case the diffraction pattern has to shift now to its original position. For 10a and 10c have to give the same setting, if the substrate is sufficiently flat. In practice the average is taken of 10a and 10c. The parameter $(n-1)d$ is known now (23) except for $m\lambda$ (m being a natural number). But in most cases m is well-known from the monitoring, so that this gives no problems.

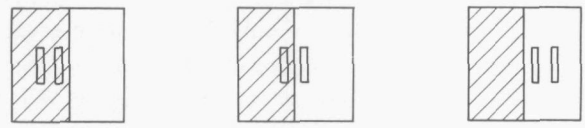

Fig. 10. Place of the substrate with respect to the double slit during the measurements. The situations a and c have to give the same adjustment.

In order to measure the constant i_p of the setup the exit slit is adjusted at one of the first order minima in the same way as above. Then the compensator is rotated through an angle i_p' so as to reach the opposite first order minimum. The angle i_p' has to be corrected according to table I. This corrected value i_p is the constant of the setup. i_p is independent of the position of the substrate with respect to the double slit.

To check whether the substrate is sufficiently plane the exit slit is adjusted at one of the first order minima as above. This minimum has to be stationary if the substrate, before being coated, is translated perpendicular to the optical axis. Then the dioptric power of the substrate is sufficiently small. Generally speaking plane-parallel glass plates and wedges can be tested in this way.

e. *Accuracy of the setup*

The optical path difference could be determined within $\lambda/300$. It is possible to improve the accuracy by a factor two, which involves a lot of extra effort, however, and also the calculation of the average of several measurements.

A number of magnesium fluoride films have been measured with this setup and also with a Savart interferometer (see I.A.1.d). These measurements indeed agree within $\lambda/300$.

The advantage of the double slit arrangement is its extreme simplicity. A disadvantage, however, is that the observations have to be done visually, which is very tiring. The fact that the luminance of the setup is rather poor necessitated the optimal accuracy being obtained with a much wider exit slit than that used by FRANÇON and

SOULIÉ in their arrangement. Moreover, this explained why only $\lambda/300$ could be obtained; this is not quite sufficient for our purposes. The optimal slit-width and accuracy we have found, agree reasonably well with the optimal step-height and accuracy which KENNEDY and BOTTEMA found in their setup with the Michelson interferometer.

The solution to our problem has been found by introducing photoelectric detection instead of visual observation.

C. Photoelectric fringe location using harmonic modulation of the diffraction pattern

Photoelectric fringe location using modulation of the fringe pattern has caused a break-through in interferometry. By this not only the way of observation is simplified, but the accuracy with which the fringe can be located is much larger. This development has caused a revival of interferometry in laboratories as well as in industries. As far as we know K. M. BAIRD [30] was the first to use modulation of the fringes, together with visual observation (1954). The modulation can be obtained in several ways. BAIRD achieved the modulation in a Fabry-Pérot etalon by harmonically modulating the pressure in an airtight chamber containing the etalon, causing harmonic modulation of the optical path length. If, under these conditions, one observes the central spot of the fringe pattern, the intensity will show flicker for most values of the average pressure in the system, if a suitable frequency is taken. However, when the average pressure is adjusted so that the oscillation is symmetrical with respect to the peak of the intensity curve, the flickering reaches a minimum. In this way BAIRD could locate the fringe within a few thousandths of the wave-length. HUNTOON, WEISS and SMITH [31] were the first to make use of photoelectric detection together with time-harmonic modulation. They achieved the modulation by a suitable vibration of one of the plates of an interferometer (Fizeau fringes). Furthermore a symmetrical slit is arranged in the image plane of the interferometer so that only an appropriate portion of the fringe field will be visible and the luminous flux through the slit will depend on the phase differences existing between the interfering light components. If the interferometer plate spacing is increased at a uniform rate the intensity will vary sinusoidally, but if one of the interferometer plates is given a small sinusoidal vibration the intensity will vary in a more complex fashion. The light passing through the image plane slit falls on a photomultiplier, which yields a voltage output proportional to the luminous flux. The signal of the photomultiplier will be a modulated wave containing the frequencies of in this case the vibrating plate and its higher harmonics.

The operation of this electrical signal to obtain a sensitive setting for the location of the fringes can be done in several ways, for instance, by phase sensitive detection. In our case we make use of the fact that the first harmonic will appear to have a zero passage and the second harmonic a maximum for the peak intensity of the central fringe.

1. *Modulation of a cosine-shaped diffraction pattern*

To determine precisely the shift Δx of the diffraction pattern, caused by a thin film, the diffraction pattern is modulated. We have achieved the modulation with the aid of a plane-parallel glass plate, placed just before the focal plane where the fringes are observed, at a suitable angle with the optical axis, causing the diffraction pattern to shift perpendicularly to the optical axis (fig. 11). Now this plate is given a uniform rotation around the optical axis with a frequency ω. Then the normal of the rotating plate describes a conical surface around the optical axis, thus about the light beam. From this it appears that the diffraction pattern attains a circular movement.

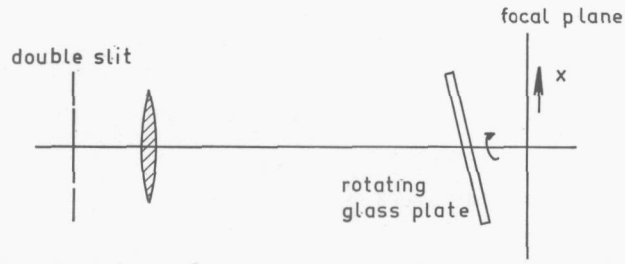

Fig. 11. The modulation is achieved by a plane-parallel glass plate, uniformly rotating about the optical axis at a suitable angle.

In the focal plane a slit has been placed parallel to the fringes and behind this slit a photomultiplier. Consequently this photomultiplier is 'seeing' only a part of the diffraction pattern moving in the form of a cosine perpendicularly to the optical axis, with a frequency ω.

To describe the modulation mathematically the intensity of the diffraction pattern, in the absence of film, can be written as (4, 7)

$$I = I_0\left[1+\cos\left(\frac{2\pi}{p}x\right)\right] \tag{24}$$

If the plate has a position such that the shift is zero, the photomultiplier will receive an intensity (fig. 12):

$$I_f = \int_{\tau-0.5b_2}^{\tau+0.5b_2} I_0\left[1+\cos\left(\frac{2\pi}{p}x\right)\right]\mathrm{d}x = b_2 I_0 + \frac{p}{\pi} I_0 \sin\frac{\pi}{p} b_2 \cos\frac{2\pi}{p}\tau \tag{25}$$

where b_2 denotes the slit-width and τ the displacement of the slit from the centre of the diffraction pattern. If the glass plate is rotating, the diffraction pattern is modulated in such a way that

$$\tau = a_0 + a\cos\omega t \tag{26}$$

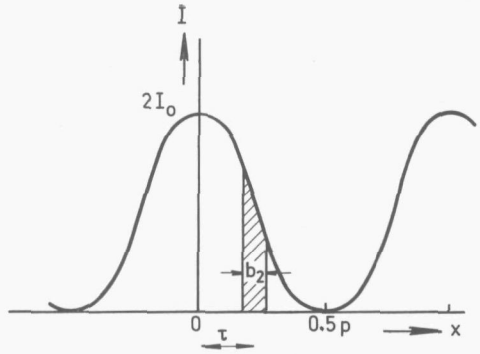

Fig. 12. The intensity I of the diffraction pattern versus the coordinate x. The photomultiplier receives only the hatched part.

where a is the amplitude of the shift caused by the glass plate. Formula (25) transforms then into

$$I_f = b_2 I_0 + \frac{p}{\pi} I_0 \sin\frac{\pi}{p} b_2 \cos\frac{2\pi}{p}(a_0 + a\cos\omega t) =$$

$$= b_2 I_0 + \frac{p}{\pi} I_0 \sin\frac{\pi}{p} b_2 \cos\frac{2\pi}{p} a_0 \cos\left(\frac{2\pi}{p} a\cos\omega t\right) -$$

$$- \frac{p}{\pi} I_0 \sin\frac{\pi}{p} b_2 \sin\frac{2\pi}{p} a_0 \sin\left(\frac{2\pi}{p} a\cos\omega t\right) \tag{27}$$

If we write [34]

$$\cos\left(\frac{2\pi}{p} a\cos\omega t\right) = J_0\left(\frac{2\pi}{p} a\right) + 2\sum_1^\infty J_{2m}\left(\frac{2\pi}{p} a\right)\cos(2m\omega t)(-1)^m \tag{28}$$

$$\sin\left(\frac{2\pi}{p} a\cos\omega t\right) = 2\sum_0^\infty J_{2m+1}\left(\frac{2\pi}{p} a\right)\cos(2m+1)\omega t(-1)^m \tag{29}$$

where J_m is a Bessel function of the m^{th} order, then (27) transforms into

$$I_f = b_2 I_0 + \frac{p}{\pi} I_0 \sin\frac{\pi}{p} b_2 \cos\frac{2\pi}{p} a_0 \cdot J_0\left(\frac{2\pi}{p} a\right)$$

$$- \frac{2p}{\pi} I_0 \sin\frac{\pi}{p} b_2 \sin\frac{2\pi}{p} a_0 \left[J_1\left(\frac{2\pi}{p} a\right)\cos\omega t - J_3\left(\frac{2\pi}{p} a\right)\cos 3\omega t + \ldots\right] -$$

$$- \frac{2p}{\pi} I_0 \sin\frac{\pi}{p} b_2 \cos\frac{2\pi}{p} a_0 \left[J_2\left(\frac{2\pi}{p} a\right)\cos 2\omega t - J_4\left(\frac{2\pi}{p} a\right)\cos 4\omega t + \ldots\right] \tag{30}$$

From (30) can be seen that the amplitude of every harmonic has a maximum if $\sin(\pi b_2/p) = 1$. Therefore the slit has been given a width equal to half of the fringe period p: $b_2 = 0.5p$.

The modulation amplitude is preferably chosen in such a way that $J_1(2\pi a/p)$ assumes its maximum because this maximum is larger than that of all other harmonics. This is illustrated for the Bessel functions of the first and second order in fig. 13.

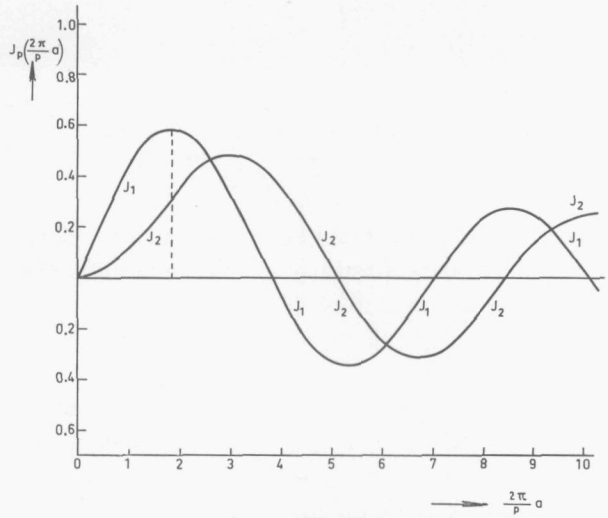

Fig. 13. The Bessel functions $J_1(2\pi a/p)$ and $J_2(2\pi a/p)$.

Therefore the signal I_f of the photomultiplier has been supplied to a selective amplifier for the first harmonic. The maximum of $J_1(2\pi a/p)$ is achieved for $2\pi a/p$ is equal to about 1.8, which corresponds to a modulation amplitude a caused by the rotating glass plate of about 0.3 of the fringe period p. The thickness of the rotating plate has been chosen 3 mm. In the same way as in the case of the compensator plate (II.B.1.b) from (20) and fig. 9, it can be calculated that the angle of incidence at the rotating plate has to be about 4°. It can be seen from (30) that if the slit is placed at a maximum or a minimum of the diffraction pattern, the first harmonic goes through zero, because $\sin(2\pi a_0/p) = 0$, whereas the second harmonic has a minimum respectively a maximum, because $\cos(2\pi a_0/p) = \pm 1$. It has turned out that this fact can be used to make precise adjustments at the central maximum of the diffraction pattern. The selective amplifier for the first harmonic of I_f has been given a selectivity such that also some part of the second harmonic passes the amplifier. In order to observe the amplified signal it has been supplied to an oscilloscope. If the slit is shifted in the direction of the central maximum of the diffraction pattern the oscillogram shows a decreasing amplitude of the first harmonic. If the slit approaches the central maximum

the first harmonic vanishes and the second harmonic becomes visible (fig. 14); if it is positioned exactly at the central maximum the first harmonic has a zero passage and then the second harmonic only is visible, giving a symmetrical oscillogram (fig. 15).

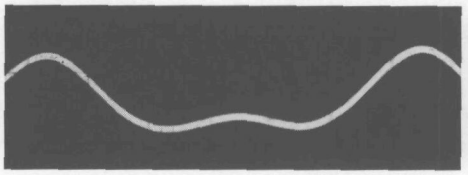

Fig. 14. The exit slit is nearly adjusted at the peak of the central fringe of the diffraction pattern.

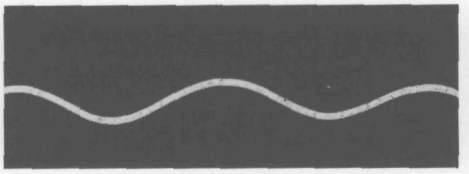

Fig. 15. The exit slit is adjusted at the peak of the central fringe of the diffraction pattern.

Due to this symmetry the adjustment can be carried out with extreme precision. So the adjustment of the slit at the central maximum of the diffraction pattern in this way yields a very accurate determination of the shift Δx of the diffraction pattern, caused by a thin film. In principle this can also be done by setting the slit at other maxima or minima of the diffraction pattern (see II.C.2).

No special attention has been paid to the phase relation between the first and second harmonic. However, the selective amplifier causes undoubtedly a phase shift between the harmonics. For a few values of such phase shifts the oscillogram has been drawn in fig. 16, viz for the case of a phase difference zero respectively 45°. Furthermore it has been supposed that the slit is maladjusted so much that the amplitudes of both harmonics are equal to each other. The reader can judge for himself, which phase difference will give the most sensitive adjustment of the slit at the central maximum of the diffraction pattern. In our opinion the phase relation between the two harmonics does not matter much.

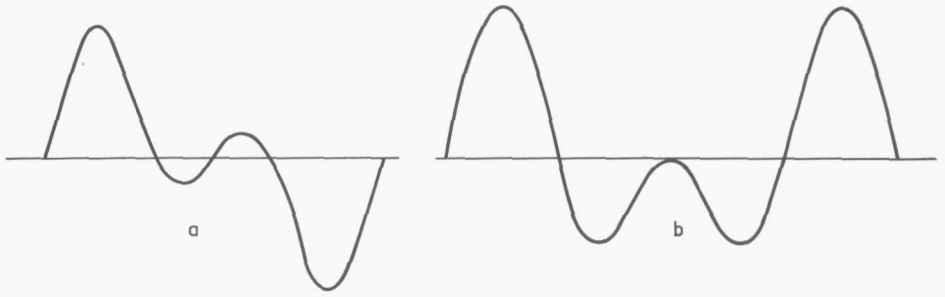

Fig. 16. The influence of the phase relation between the first and the second harmonic at the shape of the oscillogram, if the exit slit is adjusted near the central maximum of the diffraction pattern. The phase difference between the first and the second harmonic is: a. 0°; b. 45°.
The amplitude of both harmonics have been taken equal to each other.

2. *Calculations for the double slit diffraction pattern*

The intensity distribution of the diffraction pattern of a double slit is not a cosine function, but a cosine function multiplied by a sin x/x function. Moreover in practice the degree of coherence is less than unity, causing the minima to be non-zero. Besides the intensities of the two light beams, after passing through the substrate and the double slit, are not equal to each other. In most cases the cosine approximation is allowed, but in order to determine the limitations of this approximation for the present method, the intensity as a function of the coordinate x will be calculated in a more exact way.

In fact a quasi-monochromatic source is imaged at an entrance slit with width b_1 (fig. 17) in the focal plane of a lens. So a collimated beam, passing through the

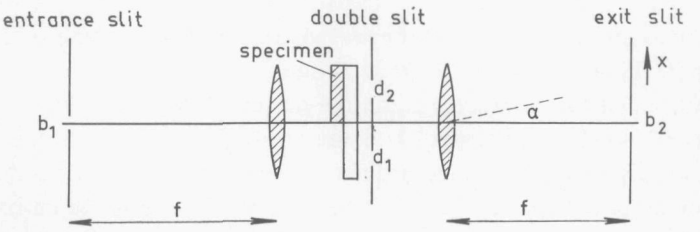

Fig. 17. The interference experiment with a double slit in a more exact way, taking into consideration the finite slitwidths of the entrance slit and the double slit.

specimen perpendicularly, is transmitted by the double slit respectively with widths d_1 and d_2 and a mutual distance between their centres h. The intensity of the diffraction pattern in the focal plane of a lens can now be written as [35]:

$$I = I_1 + I_2 + 2\mu\sqrt{I_1 I_2}\cos z \tag{31}$$

with z denoting the phase difference between the two interfering beams:

$$z = \frac{2\pi h}{\lambda f}x - \frac{2\pi}{\lambda}e \tag{32}$$

where e is again the optical path difference, caused by the thin film and where f is the focal length of the lens. I_1 is the intensity which would be observed in the focal plane of the lens if only slit 1 of the double slit were open and I_2 having a similar interpretation. μ is the degree of coherence, which is essentially positif.

If the widths of the double slit are small compared to their lengths the intensities I_1 and I_2 are respectively (Fraunhofer diffraction integral):

$$I_1 = T_1 I_{10} \left[\frac{\sin\left(\frac{\pi}{\lambda} d_1 \sin\alpha\right)}{\frac{\pi}{\lambda} d_1 \sin\alpha} \right]^2 = T_1 I_{10} \left[\frac{\sin\left(\frac{\pi d_1}{\lambda f} x\right)}{\frac{\pi d_1}{\lambda f} x} \right]^2 \tag{33}$$

$$I_2 = T_2 I_{20} \left[\frac{\sin\left(\frac{\pi}{\lambda} d_2 \sin\alpha\right)}{\frac{\pi}{\lambda} d_2 \sin\alpha} \right]^2 = T_2 I_{20} \left[\frac{\sin\left(\frac{\pi d_2}{\lambda f} x\right)}{\frac{\pi d_2}{\lambda f} x} \right]^2 \tag{34}$$

considering only small angles α (fig. 17), just like in (32). T_1 and T_2 are the transmissivity coefficients of the specimen respectively near the slit 1 and the slit 2 of the double slit, while $T_1 I_{10}$ and $T_2 I_{20}$ are the intensities at the centre of the respective diffraction patterns. Properly speaking we have neglected here the influence of the finite slit-width b_1 of the entrance slit at I_1 and I_2.

If the width b_1 of the entrance slit and the mutual distance h of the double slit are small compared to the focal length f of the lens between the entrance slit and the double slit, μ is equal to the absolute value of the normalized Fourier transform of the intensity function of the source [36]. In this case the source is the entrance slit uniformly illuminated. Besides, the width b_1 of the entrance slit is small compared to its length, so that

$$\mu = \left| \frac{\sin\left(\frac{\pi b_1}{\lambda f} h\right)}{\frac{\pi b_1}{\lambda f} h} \right| \tag{35}$$

(32), (33), (34) and (35) transform (31) into:

$$I = T_1 I_{10} \left[\frac{\sin\left(\frac{\pi d_1}{\lambda f} x\right)}{\frac{\pi d_1}{\lambda f} x} \right]^2 + T_2 I_{20} \left[\frac{\sin\left(\frac{\pi d_2}{\lambda f} x\right)}{\frac{\pi d_2}{\lambda f} x} \right]^2 + 2\sqrt{T_1 T_2 I_{10} I_{20}} \cdot$$

$$\cdot \frac{\sin\left(\frac{\pi d_1}{\lambda f} x\right)}{\frac{\pi d_1}{\lambda f} x} \cdot \frac{\sin\left(\frac{\pi d_2}{\lambda f} x\right)}{\frac{\pi d_2}{\lambda f} x} \cdot \left| \frac{\sin\left(\frac{\pi b_1}{\lambda f} h\right)}{\frac{\pi b_1}{\lambda f} h} \right| \cdot \cos\left(\frac{2\pi h}{\lambda f} x - \frac{2\pi}{\lambda} e\right) \tag{36}$$

The envelopes of the intensity function I of the diffraction pattern are found by taking

$$\cos\left(\frac{2\pi h}{\lambda f}x - \frac{2\pi}{\lambda}e\right)$$

respectively to be -1 and 1. An example of the intensity function I is given in fig. 18 for the case that $\lambda = 5461$ Å, $d_1 = d_2 = 0.350$ mm, $f = 539$ mm, $h = 1.234$ mm, $b_1 = 0.085$ mm, $T_1 = T_2 = 1$ and $e = 0$. Then the degree of coherence $\mu = 0.8$. In fact in our case the degree of coherence is higher, but $\mu = 0.8$ has been taken for the sake of clarity of fig. 18.

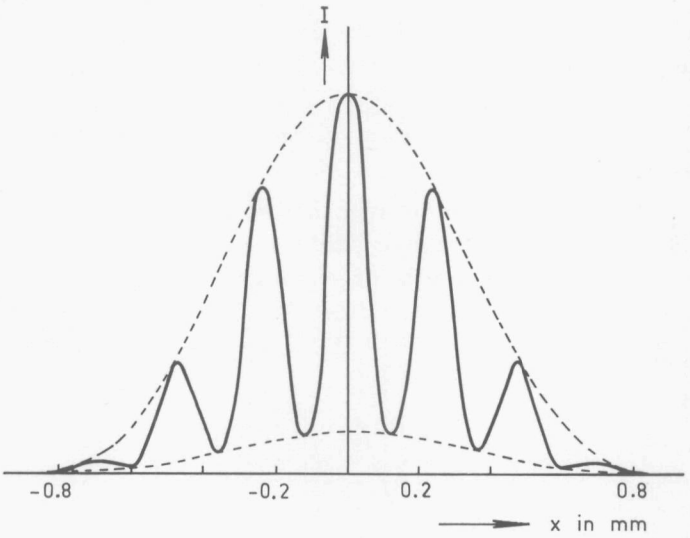

Fig. 18. Example of the intensity I of the diffraction pattern versus the coordinate x. $T_1 = T_2 = 1$; $\lambda = 5461$ Å; $d_1 = d_2 = 0.350$ mm; $\mu = 0.8$; $e = 0$.

a. *Location of the maxima and minima*

The diffraction pattern shows an absolute maximum at its centre, if the optical path difference $e = m\lambda$. Besides, then the pattern is symmetrical around its centre ($x = 0$). Therefore the central maximum of the diffraction pattern has been taken as setting point in the measurements with the modulating method.

Further from (36) it follows that the maxima and minima are not equally spaced, especially the distance of the maxima differ much from the approximated case. Which distance now has to be chosen as the equivalence of the period of the fringes, as discussed previously. Now the central maximum has been chosen as setting point, so the distance of this central maximum to the next maximum, corresponding to an optical path difference λ, has to be taken as being the 'period' of the fringes.

This 'period' of the fringes has to be measured only once, because it is independent of the thin films. Unfortunately this 'period' cannot be measured with sufficient accuracy, using the modulating method, due to the asymmetric character of the maximum next to the central maximum (see II.C.2.*c*). Therefore this has to be done visually with the method of Françon described in II.B. However, with the visual method, the slit is set at a minimum next to the central maximum, so here a minimum is used as setting point. Thus with the visual method only the distance of the two minima next to the central maximum can be measured with sufficient accuracy. What we have done actually is measuring the distance of the minima next to the central maximum with the visual method. And from this we calculated the distance of the central maximum to the successive maximum with the aid of formula (36). This distance is then the 'period' of the fringes in the phase retardation measurements with the modulating method.

b. *Influence of the degree of coherence and the intensity difference between the two wave-fronts*

From (36) it follows that the distance of the two minima lying next to the central maximum of the diffraction pattern as well as the distance of the central maximum to the next maximum depend on the degree of coherence μ in such a way that the

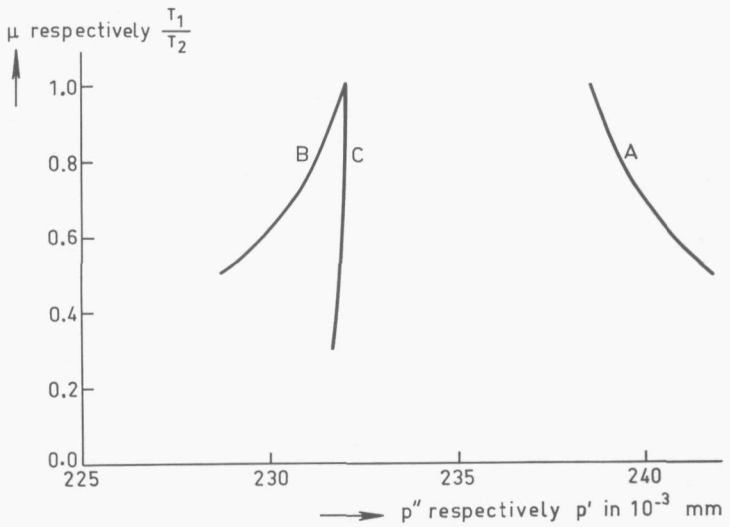

Fig. 19. A. The degree of coherence μ calculated as a function of the distance p'' between the two minima next to the central maximum.
B. The degree of coherence μ calculated as a function of the distance p' from the central maximum to its adjacent maximum.
C. The ratio T_1/T_2 of the intensities of the two interfering beams calculated as a function of p'.

distance respectively *increases* and *decreases* with a *decreasing* degree of coherence. To calculate the distance of the central to its adjacent maximum from the visual measurement of the distance of the minima lying next to the central maximum the degree of coherence μ has to be known. Taking $\lambda = 5461$ Å, $b_1 = 25.10^{-3}$ mm, $f = 539$ mm and $h = 1.234$ mm we obtain with (35) a degree of coherence $\mu = 0.97$. Fig. 19 shows the degree of coherence as a function of the distance p'' of the two minima next to the central maximum (curve A) and as a function of the distance p' from the central to its adjacent maximum (curve B) for the dimensions of our setup. The curves calculated show that the approximation, caused by taking $\mu = 1$ instead of 0.97 does not introduce an error larger than $\lambda/1000$, the accuracy of the measurements.

Further fig. 19 gives the influence of the ratio T_1/T_2 of the intensities of the two wave-fronts after passing the specimen at the distance p'. The calculated curve C shows that this influence can be neglected. Of course such a difference in intensity does cause a decrease of the modulation depth, hence a decrease in sensitivity.

Moreover from (36) it can be derived that the shift Δx of the central maximum of the diffraction pattern, caused by the optical path difference e of a thin film, depends on the degree of coherence as well as on the relative difference in intensity between the two wave-fronts. The accuracy aimed at is $\lambda/1000$. This is equal to a shift of $0.23 \cdot 10^{-3}$ mm, which is 10^{-3} of the distance p' from the central to its adjacent maximum. The systematic error, caused by the above-mentioned effects is smaller in most cases. This is illustrated in table II with a few calculated examples.

TABLE II

$2\pi e/\lambda$	μ	T_1	T_2	Δx in 10^{-3} mm	error
0.2π	1	1	1	23.20	$< \lambda/5000$
0.2π	0.8	0.5	1	23.13	$-\lambda/3400$
π	1	1	1	116.10	$+\lambda/2300$
π	0.8	1	1	115.72	$-\lambda/850$
π	0.8	0.3	1	115.37	$-\lambda/370$

Only a small correction has to be made in the last two examples. From the third example and (36) can be seen, that even if $\mu = 1$ and $T_1 = T_2 = 1$ the shift Δx as a function of the phase difference is not quite linear. A linear approximation would yield $\Delta x = 116.00$ instead of 116.10. However, this deviation can always be ignored.

c. *Influence of asymmetry of the diffraction pattern*

If there is no specimen before the double slit, the diffraction pattern is symmetrical about its centre, the coordinate $x = 0$. If we set the slit, using the modulating method, at the central maximum of the diffraction pattern, making the first harmonic of the

electrical signal zero, then indeed the exit slit will be at this central maximum, because of the symmetry of the diffraction pattern. If we try to set the slit at a maximum, lying in the slope of the envelope, the exit slit will not be exactly at this maximum, if the first harmonic of the electrical signal has a zero passage. This is caused by the fact that this maximum has no axis of symmetry (fig. 18). Consequently this will cause a systematic error in the measurement of the distance p' from the central to its adjacent maximum. It can easily be seen that this asymmetry results in the distance p' being too great. If we adjust at a minimum of the diffraction pattern the error due to asymmetry is much larger, which is obvious from fig. 18.

In order to prevent these systematic errors the distance p' has been calculated from the visually measured distance p'' between the minima next to the central maximum (see table III).

TABLE III

	calculated from (36)	measured	
		visually	modulating
distance p'' between the two minima next to the central maximum, in 10^{-3} mm	238.6 ± 0.1	238.7 ± 0.5	263.3 ± 0.5
distance p' from the central to its adjacent maximum, in 10^{-3} mm	231.9 ± 0.1	232.1 ± 0.5 *	233.6 ± 0.5

* This value has been calculated with (36) from the visually measured distance p''.

Furthermore the diffraction pattern will usually not be symmetric when measuring the optical path difference e of a thin film. This is illustrated in fig. 20 for the case that $e = \frac{3}{4}\lambda$, $\lambda = 5461$ Å, $d_1 = d_2 = 0.350$ mm, $f = 539$ mm, $b_1 = 0.085$ mm, $h = 1.234$ mm and $T_1 = T_2 = 1$. However, we always set the slit at the maximum of the diffraction pattern with the highest intensity. This maximum is always very near tot the coordinate $x = 0$. It will always be between $x = -116.10^{-3}$ and $+116.10^{-3}$ mm, whereby the amplitude of the modulation is so large that the two adjacent minima are barely involved. Under these conditions the error owing to asymmetry always remains very small. In order to check this a number of films have been measured both visually and photoelectrically. Some examples are given in table IV.

TABLE IV

	$(n-1)d$ in Å	
	visually	modulating
magnesium fluoride film	332 ± 10	333 ± 6
zinc sulphide film	941 ± 12	933 ± 1

There is a reasonable agreement between these values.

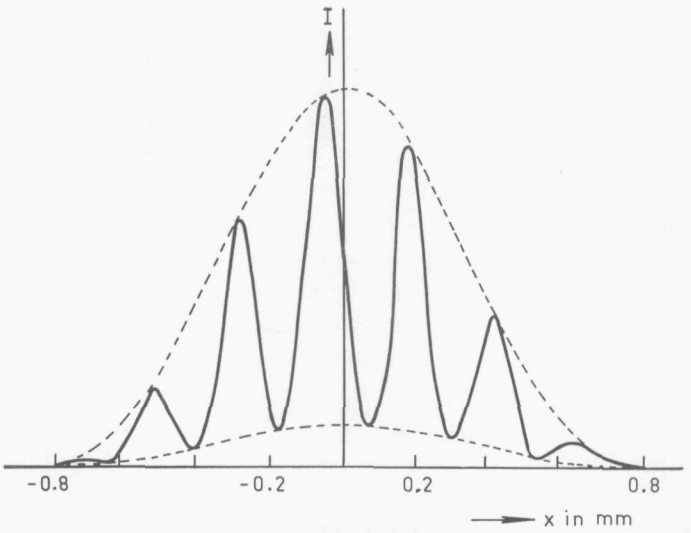

Fig. 20. Example of the intensity I of the diffraction pattern as a function of the coordinate x, whereby $e \neq m\lambda$. $T_1 = T_2 = 1$; $\lambda = 5461$ Å; $d_1 = d_2 = 0.350$ mm; $\mu = 0.8$; $e = \frac{3}{4}\lambda$.

3. *Description of various setups*

Three setups based on the above principle have been constructed: (a) a setup for measurements using transmitted light, (b) a setup using reflected light and finally (c) a setup facilitating measurements in vacuo, which latter we consider to be the most important one.

a. *Setup using transmitted light*

In a similar way as in fig. 8 (see II.B.1) the entrance slit is illuminated by a mercury lamp (fig. 21). However, all commercial mercury lamps are supplied with an AC-voltage, therefore a rectifier had to be made to eliminate the 50Hz modulation. The DC-voltage obtained showed a ripple of 0.5 V; this was harmless, because this was sufficiently suppressed by the selective amplifier.

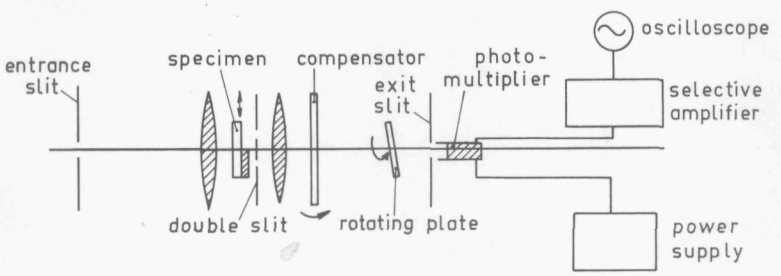

Fig. 21. Setup using transmitted light.

The collimated beam is sent through the partly coated substrate and the double slit. The diffraction pattern is formed in the focal plane of a lens. The exit slit placed in this focal plane, parallel to the fringes, with a width equal to half of the distance of two successive maxima of the diffraction pattern, is transmitting the centre of the diffraction pattern. A plane-parallel glass plate, uniformly rotating about an axis parallel to the optical axis of the setup with a frequency of 15 Hz, is modulating the diffraction pattern as is described above. A photomultiplier, fed by a high voltage power supply, detects the light transmitted by the exit slit. The signal is amplified by a selective amplifier with its peak transmission for the frequency of the rotating plate. The amplified signal is displayed on an oscilloscope.

The rotating plate is mounted in a hollow axis, permitting adjustment of its inclination. The axis is driven by means of a synchronous motor. The plate is adjusted in such a way that the amplitude a of the modulation is about 0.3 of the distance of two successive maxima of the diffraction pattern. The exact value of the modulation amplitude is not very critical, because the Bessel function $J_1(2\pi a/p)$ assumes its maximum for this case (fig. 13). Therefore the adjustment can easily be checked visually, by observing the diffraction pattern by means of a microscope, while the plate is rotated slowly by the observer.

The measurement of the optical path difference, caused by the thin film, is done in a similar way as with the visual setup (II.B.1.d). The substrate is placed as is indicated in fig. 10a. The optical compensator is placed perpendicularly to the optical axis. The exit slit is now adjusted provisionally at the centre of the diffraction pattern. After this the fine adjustment is achieved with the aid of the optical compensator. Then the undistorted second harmonic of the electrical signal appears at the oscilloscope. Now the substrate is placed as is illustrated in fig. 10b. This causes a shift Δx of the diffraction pattern. The shift is compensated by tilting the compensator plate till the undistorted second harmonic appears again. In order to eliminate eventually dioptric power of the substrate, it is placed as is illustrated in fig. 10c. In the ideal case the diffraction pattern has to shift now to its original position. In practice the average is taken of 10a and 10c.

With this setup a rapid and accurate determination of the parameter $(n-1)d$ of transparent or slightly absorbing films is possible (see III). If the transmissivity of the film is 50% or more, the absolute error can be kept within $\lambda/1200$. At lower transmissivities the accuracy decreases somewhat with the transmissivity. The measurement just described can be completed in about one minute.

b. *Setup using reflected light*

In this case a beam splitter is placed between the entrance slit and the lens (fig. 22). The specimen is placed behind the double slit. The two beams, transmitted by the double slit, are reflected by either the reflecting substrate or a flat mirror, and after that transmitted by the double slit again. The diffraction pattern is formed in the focal

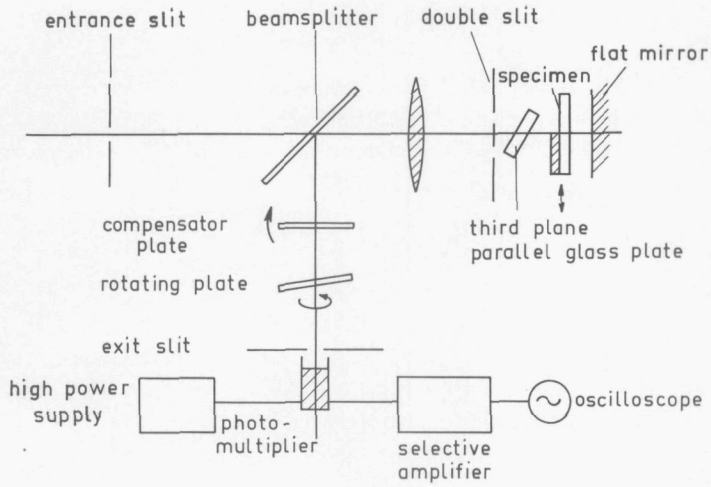

Fig. 22. Setup using reflected light.

plane of the lens by way of the beam splitter. The further components of this setup are identical to those in the setup using transmitted light. In this setup it is advisable to use a more sensitive type of photomultiplier, because the intensity of the diffraction pattern is only a fourth of that in the setup using transmitted light.

The setup can be used in several ways: the thickness d of transparent or absorbing films can be measured, if the specimen has been provided with a fully reflecting film; for transparent or slightly absorbing films on a transparent substrate, the measurement yields the parameter $(n-1)d$. If the substrate itself is reflecting, but highly absorbing and the substrate is partly coated with a transparent film, the measurement is complicated by the fact that the phase changes at the boundaries are unknown. With this setup it is also possible to keep the absolute error within $\lambda/1200$.

c. *Setup for measurements in vacuo*

In principle this setup is the same as the one described in II.C.3.a. The collimated beam, emerging from the lens, is transmitted by the double slit and passes through the specimen by way of a window and three pentaprisms in the vacuum chamber (fig. 23). The diffraction pattern is formed in the focal plane of a second lens by way of a fourth pentaprism and a second window.

The windows are plane-parallel glass plates of normal grade optical glass. A pentaprism causes a deviation of the beam of 90°; this angle is invariant, i.e. the angle does not change, if the prism is rotated around an axis perpendicular to the plane of figure 23. Consequently mechanical vibrations caused, for instance, by the vacuum pump, will have little influence on the direction of the light beam.

The film is produced in such a way that only a part of the substrate is coated. This

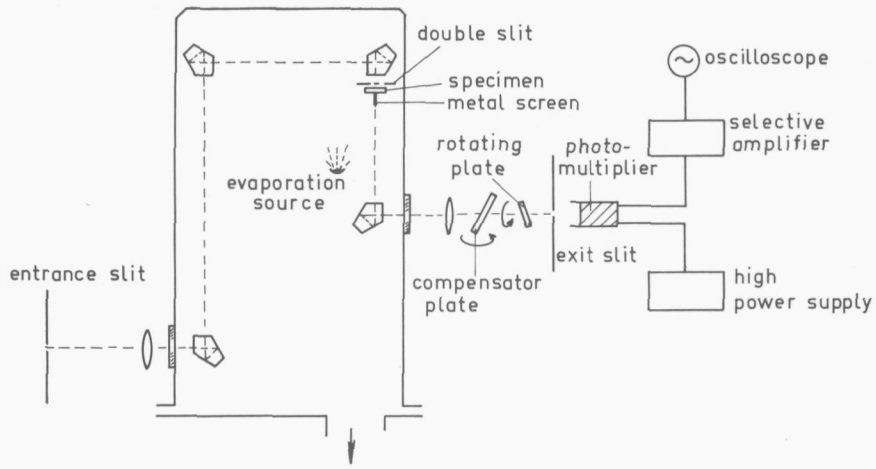

Fig. 23. Setup for measurements in vacuo.

is achieved by placing a thin metal screen perpendicular to the substrate, so that the film is deposited on the left part only, whereas the right part is uncoated. This setup can be used to measure the parameter $(n-1)d$ in vacuo as well as in air for transparent or slightly absorbing films on a transparent substrate. The absolute error can be kept within $\lambda/1000$.

d. *Accuracy of the measurements*

The errors in the measurements are caused mainly by mechanical imperfections, rather than by the inaccuracy of the adjustment of the zero passage of the first harmonic of the electrical signal. The adjustment itself can be done within $\lambda/2000$. However, the film thickness is not quite constant over the evaporation area. The thickness variations are of about 25 Å. So, the setting of the double slit with respect to the film (fig. 10) is important, because a somewhat different setting will give a somewhat different value of the measurements. The use of rather wide and long slits partly nullifies this effect.

The movement of the substrate with film in connection with the above setting is also important. This movement has to take place perpendicularly to the optical axis of the setup. If this is not the case, then it will cause a systematic error. Instead of $(n-1)d$ the transmission measurements will yield then $nd/\cos i' - d/\cos i$, i and i' being the angle of incidence respectively in air and in the film. For instance a zinc sulphide film ($nd = 0.5\lambda$) $i = 2°$ causes an error of 1 Å. The shift of the light beam, caused by tilting the substrate does not give rise to a path difference. Consequently the requirements for freedom from tilt are not very high for measurements in transmission. In the case, however, where a reflecting specimen is used, this is a different

matter, because now the direction of the light beam is changed, if the specimen tilts during the movement. A tilt of a few tenths of an arcsecond between two settings causes an error of 5 Å. This seriously affects the measurements, and necessitates a solution being found.

To solve this problem a third plane-parallel glass plate is introduced. This plate is placed between the double slit and the specimen of the setup using reflected light (fig. 22). Now the position of the specimen with respect to the double slit can be adjusted by tilting this plate around an axis perpendicular to the optical axis of the setup over an angle such that it gives the right shift. With this method the specimen can be maintained in a fixed position. This setup has proved satisfactory.

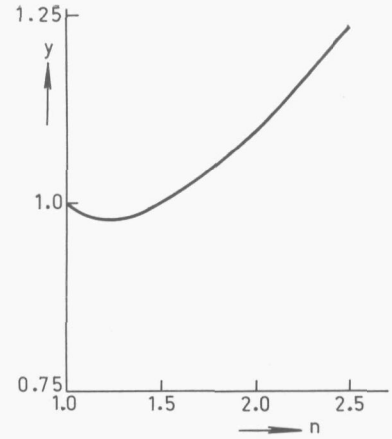

Fig. 25. $y = \dfrac{n^2+n_s}{n(n_s+1)}$ as a function of the refractive index n ($n_s = 1.52$).

ject to change after the fabrication dependent of various parameters. Then the error, made by taking the approximation $e = (n-1)d$, depends largely on the value of the parameter y in (43).

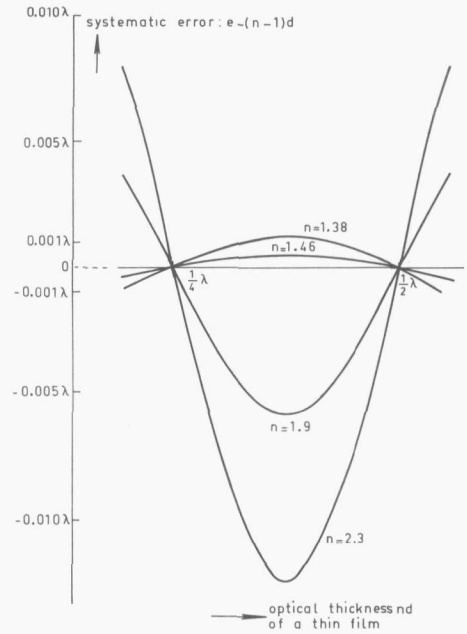

Fig. 26. The approximation $e = (n-1)d$ gives a systematic error, due to the ignorance of multiple reflections. This error $e-(n-1)d$ is calculated as a function of the optical thickness for the case of an ideal transparent film between air and a non-absorbing medium ($n_s = 1.52$).

In fig. 25 this parameter is given as a function of the refractive index of the film n; n_s has been chosen 1.52, as this is the refractive index of the substrates, which have mostly been used. It will appear, that the error for films with a refractive index between 1 and 1.52 or little above 1.52 will be small enough with respect to the accuracy of the double slit arrangement, even if the optical thickness differs much from a multiple of a quarter of a wave-length. However, for films with refractive indices much larger than that of the substrate the error becomes important. This is illustrated for a few cases in fig. 26. The error is a periodical function of the optical thickness of the film. The period is $\frac{1}{2}\lambda$. The deviation attains its maximum if $nd = (2m+1)\frac{1}{8}\lambda$, where m is a natural number. We will see in chapter V that the refractive index of thorium fluoride, for instance, can change from 1.46 to 1.55. These values are so close to n_s that the maximum error for thorium fluoride will never be larger than $\lambda/2000$. For magnesium fluoride ($n = 1.38$), however, the maximum error is $\lambda/820$. For films of cerium dioxide ($n \approx 1.9$) or zinc sulphide ($n \approx 2.3$) it is absolutely necessary to take care that the optical thickness is close enough to $nd = m\frac{1}{4}\lambda$, otherwise a correction will be necessary.

In chapter V it will appear that the changes measured in phase retardation due to various parameters are so small that if the films are evaporated such that $nd = m\frac{1}{4}\lambda$, then in practice the approximation $e = (n-1)d$ remains valid for aged films without correction.

B. An absorbing film on a transparent substrate

We consider a plane-parallel absorbing film situated between air and a transparent medium, assuming that the film is homogeneous and isotropic. Then it is possible to characterize its optical properties by means of three parameters, its thickness d, its refractive index n and its extinction index k. These last two are generally combined to form a single complex refractive index $\bar{n} = n-ik$. Now it can be shown [40], that the formula relating to the transmission of a plane monochromatic wave by the film can be obtained for normal incidence from equations (38), (39) and (40) of the above paragraph by replacing n by $\bar{n} = n-ik$. After straightforward calculation we obtain then the following formula from these expressions for the phase change δ_t on transmission:

$$\tan(\delta_t-\psi_1-\psi_s) = \frac{\left(y_1 e^{k\frac{2\pi d}{\lambda}} - y_2 e^{-k\frac{2\pi d}{\lambda}}\right)\sin\frac{2\pi\, nd}{\lambda} + y_3 e^{-k\frac{2\pi d}{\lambda}}\cos\frac{2\pi\, nd}{\lambda}}{y_3 e^{-k\frac{2\pi d}{\lambda}}\sin\frac{2\pi\, nd}{\lambda} + \left(y_1 e^{k\frac{2\pi d}{\lambda}} + y_2 e^{-k\frac{2\pi d}{\lambda}}\right)\cos\frac{2\pi\, nd}{\lambda}} \tag{44}$$

where

$$y_1 = [(1+n)^2+k^2][(n_s+n)^2+k^2]$$
$$y_2 = (1-n^2-k^2)(n^2+k^2-n_s^2)+4n_sk^2$$
$$y_3 = 2k(1+n_s)(n^2+k^2-n_s).$$

CHAPTER IV

MEASUREMENT OF THE REFRACTIVE INDEX USING THE ABELÈS METHOD

From the methods available for refractive index measurements on thin films, we chose the Brewster angle method devised by ABELÈS [8, 9], described already in chapter I, because of its elegance, simplicity and high accuracy. For measurements of the refractive index of thin films in air we adopted the setup for this method as suggested by TRAUB and OSTERBERG [42]. For measurements in vacuo we constructed a setup avoiding angular adjustments in the vacuum chamber.

A. The Abelès method

1. *Principle of the method*

If a collimated linearly polarized monochromatic light beam, polarized in the plane of incidence, is incident from air on a homogeneous isotropic film with refractive index n the reflectivity at the air-film boundary will be zero, if the angle of incidence i is equal to the Brewster angle of the film i_B. If a substrate is partly coated with a fully transparent film, then it can be shown that the reflectivity of the coated part of the substrate will be equal to the reflectivity of the uncoated part, if the angle of incidence is equal to the Brewster angle of the film i_B. This shows that the film behaves as if it were not present. This is evident from the fact that the incident wave does not find any discontinuity at the air-film boundary. In other words, we may say that the impedances of the air and the film are the same for this angle of incidence.

This provides a very simple method for the measurement of the refractive index of thin films. It is obvious that this method is only valid for isotropic homogeneous non-absorbing films. Since the condition of equal reflectivity, $n = \tan i_B$, is completely independent of the optical properties of the substrate, this method can be used for films at any substrate; in particular the substrate may be made of absorbing as well as non-absorbing material. It will be seen from the following that the sensitivity of the method, however, depends on the optical parameters of the film as well as on those of the substrate.

2. *Sensitivity of the method*

Just like the setting criterion of FRANÇON, described in II.B, the criterion used in the ABELÈS method consists in the comparison of two luminances; in other words, it is a photometric setting criterion.

The discussion of the ABELÈS method can be facilitated by formally introducing an air film with vanishing thickness between the film and the substrate. This situation is physically equivalent to the case we have in reality, i.e. the film and substrate are in optical contact (see fig. 28). A collimated beam, linearly polarized in the plane of incidence, is incident on the specimen. If the angle of incidence is equal to the

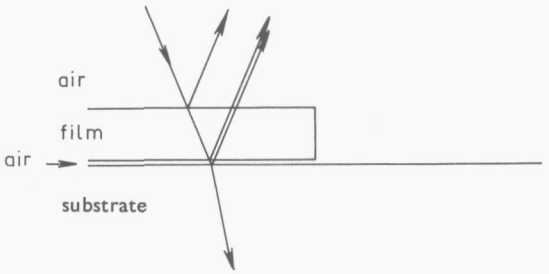

Fig. 28. The ABELÈS method can be discussed in a simple way by formally introducing a thin air film with vanishing thickness between the substrate and the film.

Brewster angle of the film then the reflectivity at the two film boundaries will be zero, so it is immediately obvious that the reflectivity is equal to that of the substrate. Let the refractive index n of the film increase with Δn, keeping the angle of incidence constant, then this increase will cause a change Δr_1 in the amplitude reflection coefficient r_1 of the air-film boundary; as the latter is given by:

$$r_1 = \frac{\tan(i-i')}{\tan(i+i')} \tag{46}$$

where i is the angle of incidence in air and i' the angle of refraction in the film, we have

$$\Delta r_1 = -\frac{\dfrac{\tan(i+i')}{\cos^2(i-i')} + \dfrac{\tan(i-i')}{\cos^2(i+i')}}{\tan^2(i+i')} \frac{\mathrm{d}i'}{\mathrm{d}n} \cdot \Delta n \tag{47}$$

The substitution $i = i_B$ transforms (47) into

$$\Delta r_1 = -\tan(i-i') \frac{\mathrm{d}i'}{\mathrm{d}n} \Delta n \tag{48}$$

The factor $\mathrm{d}i'/\mathrm{d}n$ is found from Snell's law:

$$\frac{\mathrm{d}i'}{\mathrm{d}n} = -\frac{1}{n^2} \tag{49}$$

desired this decrease in sensitivity can be prevented by taking a suitable absorbing material for the substrate or by blackening the rear of the substrate.

3. *Slightly absorbing films*

The condition for equal reflectivity of the coated and uncoated parts of the substrate is based on the assumption that the film shows no absorption. In the presence of slight absorption two important facts have to be considered. In the first place we can assume that the reflectivity of the coated part of the substrate will be below that of a fully transparent film, due to the absorption in the film itself. However, if the refractive index of the film is in the region of that of the substrate a further effect becomes important, viz in the case of an absorbing film the reflectivity at the air-film boundary due to an imaginary component in the reflectivity never becomes zero, so fundamentally there is no Brewster angle in this case. Of course we can define the angle for which the reflectivity becomes a minimum as the Brewster angle. According as the Brewster angle of the film and that of the substrate are more close to each other this effect becomes more important and will even nullify the first mentioned effect. It can be shown that in the case of small k values a systematic error arises, approximated by

$$\Delta n = \frac{k^2\left(\frac{1}{n} - \frac{1}{n^3}\right)^2}{r_s} - \frac{2\pi k}{n} \cdot \frac{r_s}{2\left(\frac{1}{n} - \frac{1}{n^3}\right)} \tag{58}$$

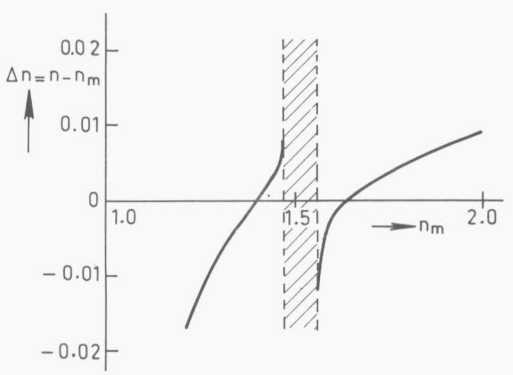

Fig. 29. The computed error $\Delta n = n - n_m$ in the refractive index n of the film, due to absorption in the film, versus the measured value n_m of the refractive index. The extinction index $k = 0.02$ and the refractive index of the substrate $n_s = 1.52$. The optical thickness has been chosen such that $nd \cos i_B' = \frac{1}{4}\lambda$.

Formula (58) reveals that for a small refractive index range, it goes so far that the ABELÈS method is practically useless because the first term becomes very large. Instead of (58) for the calculations, however, we preferred to use a regious computation with the aid of a computer. In figure 29 the computed error $\Delta n = n - n_m$ is shown versus the measured value n_m of the refractive index of the film n. The extinction index k has been chosen 0.02, the refractive index of the substrate $n_s = 1.52$ and the optical thickness of the film such that $nd \cos i_B' = \frac{1}{4}\lambda$. In the hatched area $1.48 < n < 1.56$ the ABELÈS method clearly makes no sense.

4. *Setup for refractive index measurements in air*

The measurement is most conveniently made on an ordinary goniometer using a monochromator as light source. The source is imaged on the entrance slit of the collimator and the specimen is mounted vertically on the table of the goniometer. A polarizer is put between the specimen and the telescope. One difficulty is that the telescope must be focused on the specimen while the brightness match is being made, whereas it must be focused on the entrance slit when an angular reading is to be taken. Another difficulty is the tracking of the reflected beam as the angle of incidence is varied while making the brightness match.

These difficulties are solved in the arrangement suggested by TRAUB and OSTER-

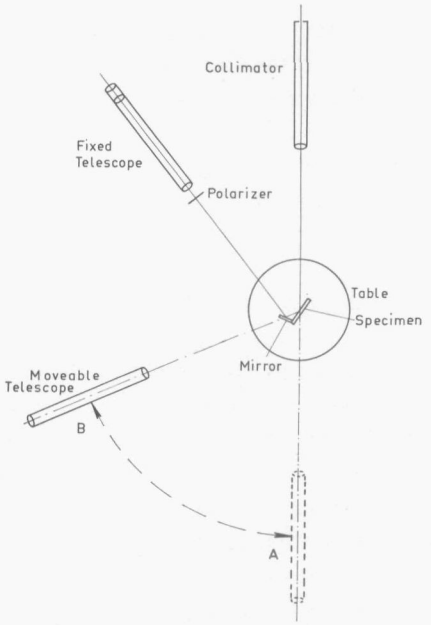

Fig. 30. Setup for refractive index measurements with the ABELÈS method.

BERG [42]. An auxiliary first-surface mirror is mounted on the specimen holder in a vertical plane making an angle of about 110° with the plane of the specimen (fig. 30). The mirror and specimen form a constant-deviation reflector so that a fixed telescope may be used for receiving the doubly reflected light. This fact introduces a new difficulty, for if the location of the slit image is insensitive to the angular position of the table of the goniometer, it cannot be used for the initial orientation of the goniometer circle. Therefore, contrary to the fixed telescope which is focused on the specimen, a second telescope is focused on the entrance slit at infinity and is rotatable round the axis of the goniometer. In order to zero the goniometer circle, the entrance slit is imaged on to the reticle of the moveable telescope at position A, with the specimen removed. The angular position of the goniometer circle is recorded. The specimen is then mounted and the moveable telescope is rotated through a measured angle to such a position (B), as to permit interception of the singly reflected rays, which pass the edge of the auxiliary mirror. The goniometer table is then rotated until these rays are intercepted by the telescope. When the slit is again imaged on the reticle the goniometer table is clamped to the goniometer circle. The apparatus is now ready for use.

The precision of the goniometer is amply sufficient for the measurement.

B. Adaptation of the Abelès method for the use in vacuo

Starting with the adaptation of the ABELÈS method for the use in vacuo, we decided that it would be very convenient if the accurate angular adjustment could be done outside the vacuum chamber whilst the specimen in the vacuum chamber is kept in a fixed position. In this case one simplification in comparison with the above described setup is possible: as the refractive index to be measured in vacuo is approximately known from measurements carried out in air with the setup described above, the angular range for the measurements in vacuo can be small.

1. *Avoidance of angular adjustments in the vacuum chamber*

A ground glass illuminated by quasi-monochromatic light acts as a diffuse light source. The ground glass is placed in the focal plane of lens L_1 (fig. 31). So a collimated beam, with a certain angular spread, passing a plane-parallel optical glass window in the bell jar, is reflected respectively by the specimen and an auxiliary first-surface mirror in the vacuum chamber. The specimen and the auxiliary mirror are placed perpendicularly to each other, acting together as a mirror with a constant deviation of 180°. So the direction of every ray is reversed by the double reflection and the beam is focused in the focal plane of lens L_1. Every point in this focal plane corresponds to a certain angle of incidence on the substrate. If a very narrow slit is now placed in this

focal plane perpendicular to the optical axis and parallel to the plane of the specimen, then only light incident under a determined angle with the substrate will pass through this slit. So the angle of incidence on the specimen of the light passing the slit is varied by shifting the slit perpendicularly to the optical axis.

However, during the variation of the angle of incidence which is done by shifting the slit, the eye behind the slit has to observe the specimen making the brightness match. Now the admissible slitwidth depends on the tolerance in the angle of incidence in connection with the accuracy desired of the measurement of the refractive

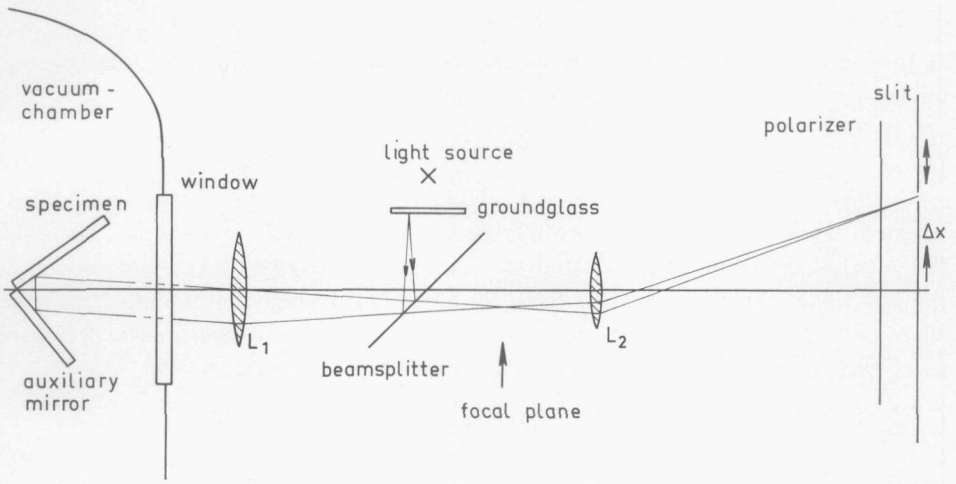

Fig. 31. Avoidance of angular adjustments in the vacuum chamber with the aid of a diffuse light source and a narrow slit.

index. A tolerance in the refractive index of about 0.001 corresponds with a slit-width of about 0.06 mm, if the focal length of the lens is 200 mm. This makes the observation of the specimen very difficult. Therefore the focal plane of the lens L_1 is imaged five times magnified by a second lens L_2.

The slit is now placed in the new image plane instead of in the focal plane of the lens L_1. The admissible slit-width then becomes 0.3 mm. The components have been chosen in such a way that the specimen is imaged just behind the second lens which decreases the vignetting. This is important, because the vignetting limits the angular range that can be covered by shifting the slit. Besides the field of view is larger in this case. The polarizer is placed in front of the slit.

In connection with the changes to be measured in the refractive index at least an angular range covered by shifting of the slit of 2° is required. Besides the field of view has to be large enough so as to ensure that a suitable part of the specimen can be observed. This has been realized with the following components and distances: the focal

length of lens L_1 ($\varnothing$ 5 cm) is 20 cm, the focal length of lens L_2 ($\varnothing$ 3 cm) is 8 cm, the distance of the specimen to lens L_1 is 40 cm, the distance of the two lenses is 29.5 cm.

A disadvantage of this setup with respect to the setup for measurements in air is that the eye has to move with the slit, while this is shifted for making the brightness match. Moreover, the luminance is reduced by the beam splitter by a factor four and by the fact that the pupil of the observer's eye is not completely filled.

2. *Detailed description of the setup*

a. *The angle of incidence on the specimen*

In this setup the angle of incidence on the specimen to be measured, i.e. the Brewster angle for the film i_B, is composed of two angles.

$$i_B = 90° - (\beta_1 + \beta_2) \tag{59}$$

where β_1 is the acute angle between the specimen and the axis of the setup. The angle $(90° - \beta_1)$ is chosen equal to the Brewster angle which may be expected to depend on the film under examination. This Brewster angle is approximately known from measurements carried out with the setup in air. The angle β_2 is measured in the setup described above by shifting the slit while making the brightness match.

$$\beta_2 = \arctan \frac{\Delta x}{uf} \tag{60}$$

where Δx is the distance from the centre of the slit to the axis, f the focal length of lens L_1 and u the magnification caused by lens L_2. So in fact in this setup the previously chosen angle β_1 is corrected by the measurement of β_2. To obtain the accuracy required in the refractive index measurement, the alignment of the setup has to take place within 1′.

b. *Adjustment of the setup*

To adjust the angle β_1 between the specimen with auxiliary mirror and the axis of the setup a plane reference mirror is mounted adjustably with respect to the specimen. Now on a goniometer the angle between the specimen and this reference mirror is adjusted at $90° - \beta_1$. In this fixed position the specimen with auxiliary and reference mirror is placed in the vacuum chamber. Now in practice the ground glass is imaged in the focal plane of the lens L_1 with the aid of a condensor.

Fig. 32 gives a sight from above at the complete setup. A reticle is placed as accurately as possible at the optical axis in the focal plane of lens L_1. The reference mirror images the reticle in both focal planes via the beam splitter. Now the reference mirror

is adjusted in such a way that the reticle image coincides with the reticle itself. The reticle is also imaged by lens L_2 in the plane of the slit. The place of this reticle image is the zero position of the slit, because the specimen makes an angle β_1 with the axis defined by the reticle and its image. The fact that this axis only coincides approximately with the optical axis of lens L_1 is no objection. A further image of the reticle

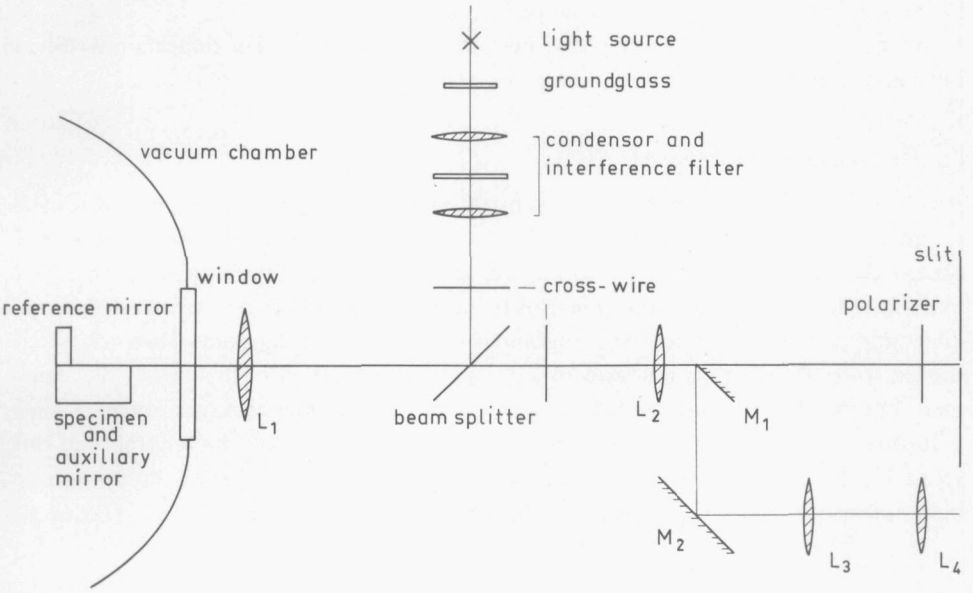

Fig. 32. View from above at the setup for refractive index measurements in vacuo.

is formed in the focal plane of lens L_1 via the specimen and the auxiliary mirror. However, if the specimen and the auxiliary mirror are not perpendicular to each other, there will be two reticle images. This can be corrected by tilting the auxiliary mirror till the reticle images coincide.

The specimen together with the auxiliary mirror and the reference mirror is placed in the vacuum chamber; hence it is mechanically isolated from the other part of the setup. In practice it appeared to be necessary to be able to check the adjustment of the reference mirror with respect to the setup at any moment during the measurements. For this purpose a second reticle is placed in the focal plane of lens L_1 behind the beam splitter and this reticle is adjusted at the image of the first reticle. If the direction of the reference mirror changes, the reticle image will displace. The reticles are imaged at infinity with the aid of the mirrors M_1 and M_2 and the lenses L_3 and L_4 (fig. 32). In this way a possible displacement of the reticle image can be checked at any moment.

c. *The specimen holder*

For reasons described above the auxiliary mirror and the reference mirror are made adjustable with respect to the specimen and with respect to each other. The substrate is only partly coated . This is achieved by shielding the auxiliary mirror and a part of the substrate during the evaporation. After the evaporation the shield is removed magnetically. The shielding can also be achieved by placing a screen perpendicular to the substrate parallel to the plane of incidence.

In most cases plane glass plates have been used as substrates. The material was either normal grade optical glass or black glass.

d. *The measuring procedure*

After the angular adjustment of the substrate and the reference mirror with respect to each other and the alignment of the setup as described above, the substrate is coated the film thickness being so chosen as to obtain a maximum sensitivity (see IV.A.2). After evaporation the shield in front of a part of the specimen and the auxiliary mirror is removed and the alignment of the setup is checked. Then the slit is shifted from its zero position adjusting at equal reflectivity of both sides of the specimen. During this measurement the alignment can be checked at any moment.

In this way the refractive index can be measured within 0.003. The reliability of this setup was checked by measuring the same specimen under the same conditions in both setups, previously described in this chapter.

CHAPTER V

MEASUREMENTS

A. Introduction

The purpose of the measurements was to obtain quantitative data concerning the change of the optical parameters n and $(n-1)d$ of thin dielectric films due to aging. In particular the influence of air on these films is examined. From these measured changes in $(n-1)d$ and n the change in d could be calculated. It is very important to know these changes, because the optical properties of a thin dielectric film are determined by the optical thickness and the refractive index; once these changes are known the operator can correct these changes by producing a coating in vacuo with a predetermined deviation from the values desired.

The number of factors which may influence the optical properties of a film formed by evaporation is considerable. Among the more obvious of these factors are: pressure in the vacuum chamber, rate of deposition, nature and temperature of the substrate, properties of the evaporate in the vapor phase, crystal form and growth habit, purity and physical state of evaporate, evaporation temperature, angle of incidence of molecules on surface, cleaning procedure of the substrate, temperature and moisture content of the air, where the film is used. In view of this complexity, it is hardly surprising that the results from different workers show some variability. In particular in much early work the experimental conditions have either not been properly controlled or have not been reported, so that inconsistencies appeared. Therefore in the measurements to be discussed, the experimental conditions which may influence film properties are reported as much as possible.

We wish to stress that we are primarily interested in the changes measured in the optical parameters $(n-1)$ and n and that we will not try to discuss the fundamental nature of these changes. Moreover we have restricted ourselves to dielectric films commonly used in optics. We measured mainly the aging influence of air on these parameters. This is done for different deposition rates and for different pressures in the vacuum chamber. We have tried to keep all other experimental circumstances the same for all the measurements. We will specify these experimental circumstances in the following section.

1. *Experimental conditions*

A good quality optical glass $n_s = 1.52$ (Schott BK 7) was mostly used for the substrates. A number of refractive index measurements have been done using substrates of black glass ($n_s = 1.52$). This improved the accuracy according to IV.A.2. The changes measured in n appeared to be the same. All substrates are ground and polished

in the optical shop. Before mounting in the vacuum chamber (Balzers BA 500) the substrates were cleaned with *T*-pol. After mounting in the vacuum chamber first a glow discharge was applied for about ten minutes at a pressure of about 10^{-2} mm Hg. Then the substrate was partly coated under a certain pressure in the vacuum chamber and with a certain deposition rate. In most cases the material was evaporated from a tantalum boat. The angle of incidence of the vapor stream on the substrate was smaller than ten degrees. The substrates were never heated before the evaporation.

Immediately after the evaporation the optical parameters were measured for $\lambda = 5461$ Å as described in chapter II and IV. Within a quarter of an hour after the evaporation dried air was admitted into the vacuum chamber till the outside pressure was obtained. After this the optical parameters were measured again. Then the vacuum chamber was opened and the measurements were repeated. All this takes place within half an hour after the evaporation. Immediately after this last measurement the specimen was removed from the vacuum chamber and the measurement was repeated making use of the setup outside the vacuum chamber. Dependent on the measured changes in the optical parameters the measurements were repeated for approximately half a year. Some change in the temperature and humidity of the surrounding air, could not be avoided. The temperature varied between 20 °C and 25 °C and the relative humidity between 45% and 55%.

The parameter $(n-1)d$ was measured within 5 Å and the parameter n within 0.003, except in a few cases where the accuracy was somewhat lower.

The coating materials were supplied by Balzers. As a matter of fact the purity of the materials differs strongly from manufacturer to manufacturer. Films consisting of the following materials were examined: magnesium fluoride (MgF_2), thorium fluoride (ThF_4), kryolite (Na_3AlF_6), lithium fluoride (LiF), zinc sulphide (ZnS), cerium dioxide (CeO_2) and silicon monoxide (SiO).

B. Results of the measurements

1. *Magnesium fluoride films*

According to the above section the changes in the optical parameters can be separated into two parts, viz more or less abrupt changes in $(n-1)d$ and n on admitting dry air and moist air in the vacuum chamber and further gradual changes as a function of time. These effects are given respectively in table V and figure 33 in dependence on the pressure during the evaporation and the deposition rate. In fact fig. 33 is a continuation of table V, with the exception of the dotted lines. These dotted lines represent films that are kept in vacuo at a pressure of 10^{-3} mm Hg for the first two days after the evaporation.

Table V and fig. 33 show that the largest change of the optical parameters $(n-1)d$ and n takes place before the film is removed from the vacuum chamber. According as

TABLE V

magnesium fluoride films	evaporation-pressure in mm Hg	deposition rate in Å/s	$(n-1)d$ in Å			n		
			vacuum	dry air	moist air	vacuum	dry air	moist air
a	10^{-5}	50	263	280	290	1.342	1.368	1.381
b	10^{-5}	50	316	337	342	1.350	1.370	1.378
c	10^{-5}	50	417	455	462	1.344	1.370	1.380
d	10^{-4}	3	274	307	312	1.305	1.354	1.373

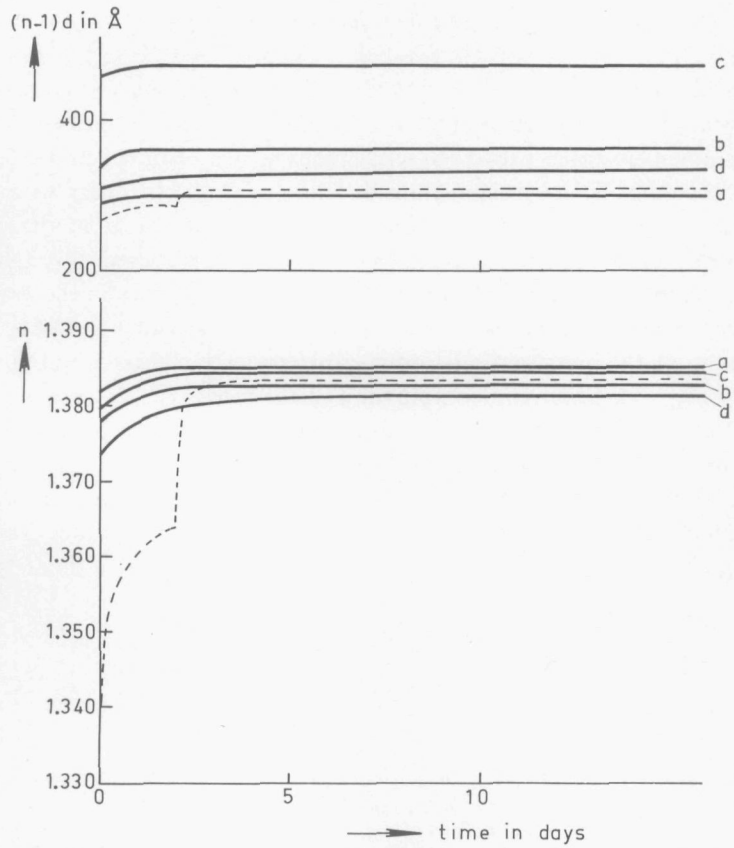

Fig. 33. Measured aging effects in the parameters $(n-1)d$ and n of magnesium fluoride films. This figure is a continuation of Table V. Time zero corresponds with the first measurement in moist air. The films corresponding with the dotted lines are kept in vacuo at a pressure of 10^{-3} mm Hg for the first two days after the evaporation. Their deposition rate was 50 Å/s and the pressure during the evaporation 10^{-5} mm Hg.

the evaporation pressure increases and the deposition rate decreases the time that the parameters $(n-1)d$ and n reach a constant value increases. The refractive index n just after the evaporation lowers, if this pressure increases and the deposition rate decreases. However, all aged films have nearly the same refractive index.

The thickness d as calculated from $(n-1)d$ and n does not change significantly, taking into account an error of 3%. Here it must be noted, however, that in the vacuum chamber $(n-1)d$ and n are measured for different specimens, evaporated under similar conditions. Furthermore fig. 33 might seem to suggest that n reaches its constant value after a longer time than $(n-1)d$. This must be attributed, however, to the way in which the $(n-1)d$ curve is drawn through the measured points.

2. *Thorium fluoride films*

The refractive index of thorium fluoride films is about 1.5, hence it is impossible to use a substrate with a refractive index $n_s = 1.52$. Therefore the measurements were done using either substrates with a refractive index $n_s = 1.65$ or substrates ($n_s = 1.52$) coated all over with a magnesium fluoride film ($nd = \frac{1}{4}\lambda$) in order to modify the effective refractive index of the substrate. For the measurement of the parameter $(n-1)d$ substrates with a refractive index $n_s = 1.52$ were used throughout. The measurements are shown in Table VI and fig. 34. The solid lines in the graph of the refractive index show the measurements using substrates with $n_s = 1.65$, while the dotted lines show the measurements using substrates with a magnesium fluoride film as undercoating. The figure is a continuation of the table.

Table VI and fig. 34 show that the total changes in the optical parameters $(n-1)d$ and n of thorium fluoride films are about twice as large as those of magnesium fluoride films. About a third part of the change takes place outside the vacuum chamber.

The graph of the refractive index versus the time shows that thorium fluoride films with a magnesium fluoride film as undercoating seem to obtain ultimately a some-

TABLE VI

thorium fluoride films	evaporation-pressure in mm Hg	deposition rate in Å/s	$(n-1)$d in Å			n					
			$n_s=1.52$			$n_s=1.65$			$n_s=1.52$+magnesium fluoride as undercoating		
			vacuum	dry air	moist air	vacuum	dry air	moist air	vacuum	dry air	moist air
a	10^{-5}	40	463	492	519	1.474	1.497	1.526	1.487	1.508	1.533
b	10^{-5}	20	606	619	687	1.468	1.496	1.525	1.472	1.494	1.527
c	10^{-5}	7	562	594	661	1.464	1.491	1.527	1.472	1.495	1.526
d	10^{-4}	6	1035	1070	1210	1.441	1.472	1.522	1.455	1.477	1.520

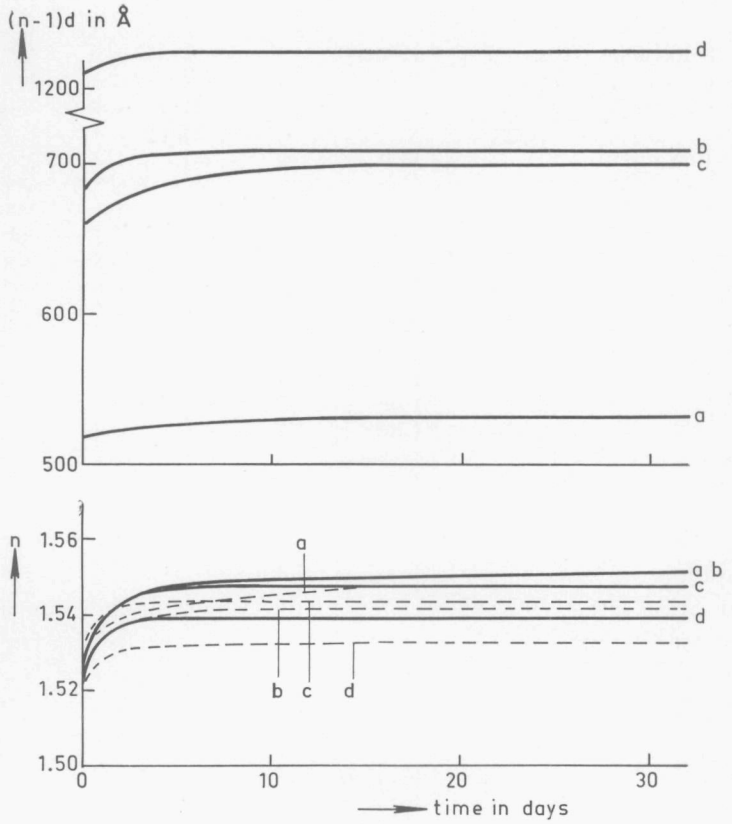

Fig. 34. Measured aging effects in the parameters $(n-1)\,d$ and n of thorium fluoride films. The figure is a continuation of Table VI. Time zero corresponds with the first measurement in moist air. The solid lines in the graph of the refractive index show the measurements on substrates with $n_s = 1.65$, while the dotted lines show those on substrates with a magnesium fluoride film as undercoating.

what lower refractive index than films on substrates with $n_s = 1.65$. It may be that this measured difference is due to aging of the undercoating.

Here also the geometrical thickness d as calculated from the measured values of $(n-1)d$ and n does not substantially change with time. This means that the change in $(n-1)d$ is mainly caused by a change in n.

3. *Kryolite films*

The measurement of the optical parameters $(n-1)d$ and n of kryolite films were made on substrates with a refractive index $n_s = 1.52$. The results are given in table VII.

TABLE VII

kryolite films	evaporation pressure in mm Hg	deposition rate in Å/s	$(n-1)d$ in Å					
			vacuum	dry air	moist air	1 day	7 days	30 days
a	10^{-5}	60	350	356	348	350	356	346
b	10^{-5}	25	586	636	625	625	629	617
c	10^{-4}	60	567	578	577	581	585	576
d	10^{-4}	25	565	617	608	612	598	606
e	10^{-5}	40	1056	1146	1150	1148	1149	1144
			n					
a	10^{-5}	60	1.315	1.318	1.314	1.318	1.317	1.317
b	10^{-5}	25	1.310	1.321	1.324	1.314	1.314	1.306
c	10^{-4}	60	1.296	1.317	1.313	1.304	1.312	1.306
d	10^{-4}	25	1.294	1.339	1.332	1.338	1.339	1.333

The aging effects can be ignored in the case of films evaporated at low pressure and high deposition rate, and having an optical thickness equal to $\frac{1}{4}\lambda$ (these conditions occur in practical cases). Only when increasing the evaporation pressure and decreasing the deposition rate slight aging effects occur. In this case $(n-1)d$ and n increase after the admittance of dry air in the vacuum chamber.

4. *Lithium fluoride films*

The measurement of the optical parameters $(n-1)d$ and n of lithium fluoride films were made using substrates with a refractive index $n_s = 1.52$. The results are given in table VIII and fig. 35.

The aging effects on lithium fluoride films appear to be less consistent than those on the films discussed in the above sections. There is a considerable change in $(n-1)d$ and n immediately after the admittance of moist air to the film. But the largest part of

TABLE VIII

lithium fluoride films	evaporation-pressure in mm Hg	deposition rate in Å/s	$(n-1)d$ in Å			n		
			vacuum	dry air	moist air	vacuum	dry air	moist air
a	10^{-5}	40	269	270	282	1.249	1.254	1.313
b	10^{-5}	20	235	233	283	1.250	1.253	1.288
c	10^{-5}	8	384	380	402	1.247	1.250	1.277
d	10^{-4}	40	220	225	271	1.240	1.242	1.283

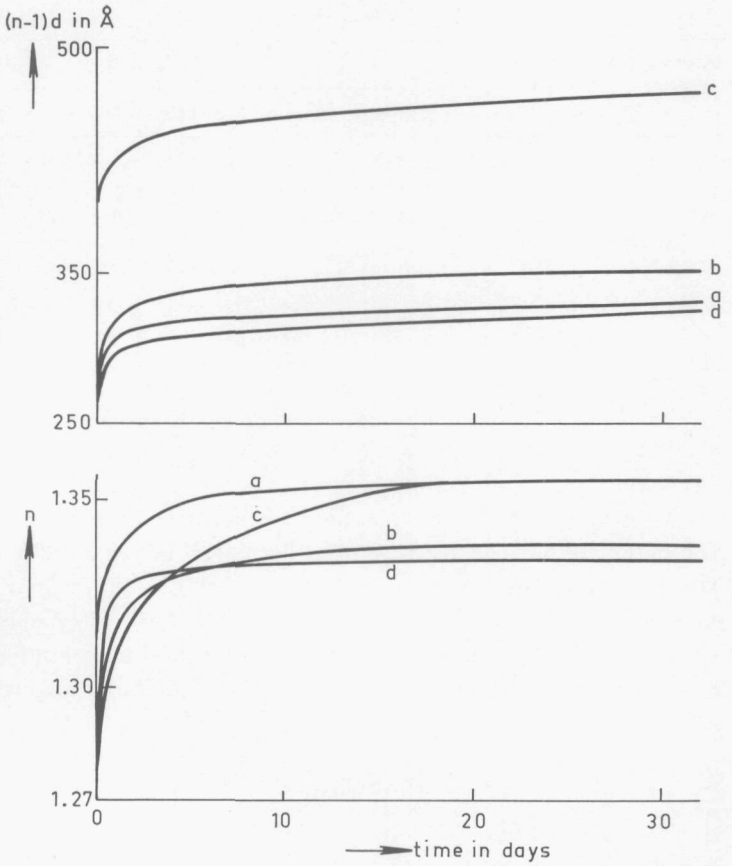

Fig. 35. Measured aging effects in the parameters $(n-1)d$ and n of lithium fluoride films. The figure is a continuation of Table VIII. Time zero corresponds with the first measurement in moist air.

the change takes place after removal of the specimens from the vacuum chamber. Moreover, this lasts for about a month.

In the first week after the evaporation the relative change in n is mostly much larger than that in $(n-1)d$, which means that the thickness d decreases with age.

5. *Zinc sulphide films*

Aging effects of zinc sulphide films appear to depend strongly on the conditions during the evaporation. We have obtained consistent data for zinc sulphide films evaporated from a closed tantalum boat, having holes at the upper side with a diameter of about 1 mm. Measurements on films deposited in such a way are given in table IX, from

TABLE IX

zinc sulphide films	evaporation-pressure in mm Hg	deposition rate in Å/s	$(n-1)d$ in Å					
			vacuum	dry air	moist air	1 day	7 days	30 days
a	10^{-5}	25	787	796	790	792	783	780
b	10^{-5}	4	803	805	800	806	795	800
c	10^{-4}	3	853	847	857	852	850	845
			n					
a	10^{-5}	25	2.335	2.335	2.339	2.340	2.336	2.337
b	10^{-5}	4	2.328	2.329	2.333	2.333	2.330	2.331
c	10^{-4}	3	2.276	2.280	2.290	2.288	2.285	2.284

which it can be seen that these films show practically no aging effects for $(n-1)d$ as well as for n.

However, if we evaporate from an open tantalum boat no consistent data could be obtained. The parameter $(n-1)d$ of these films decreases, but in a different way for each film. Some examples are shown in table X.

HALL and FERGUSON [43] encountered the same difficulty. They obtained consistent data only if the zinc sulphide was preheated in vacuo for an hour at approximately 900 °C and then for about 10 minutes at 1400 °C. They observed no aging effects.

TABLE X

zinc sulphide films	evaporation-pressure in mm Hg	deposition rate in Å/s	$(n-1)d$ in Å				
			vacuum	dry air	moist air	1 day	7 days
a	10^{-5}	30	860	852	847	812	809
b	10^{-4}	30	1287	1272	1280	1275	1259
c	10^{-4}	30	1296	1211	1225	1223	1216

6. *Cerium dioxide films*

The melting point of cerium dioxide is rather high (1950 °C). Therefore a tantalum boat cannot be used as an evaporation source. We used a tungsten boat. The results of the measurement of the optical parameters $(n-1)d$ and n of cerium dioxide films using substrates with a refractive index $n_s = 1.52$ are shown in table XI and fig. 36.

In comparison with the different kinds of films discussed up to now, the change in the parameters $(n-1)\ d$ and n of cerium dioxide films is great. Moreover, the value of the refractive index n immediately after the evaporation as well as that obtained

TABLE XI

cerium dioxide films	evaporation-pressure in mm Hg	deposition rate in Å/s	$(n-1)d$ in Å			n		
			vacuum	dry air	moist air	vacuum	dry air	moist air
a	10^{-5}	10	648	729	734	1.836	1.924	1.978
b	10^{-5}	10	621	685	718	1.809	1.885	1.957
c	10^{-4}	5	773	795	842	1.795	1.837	1.875

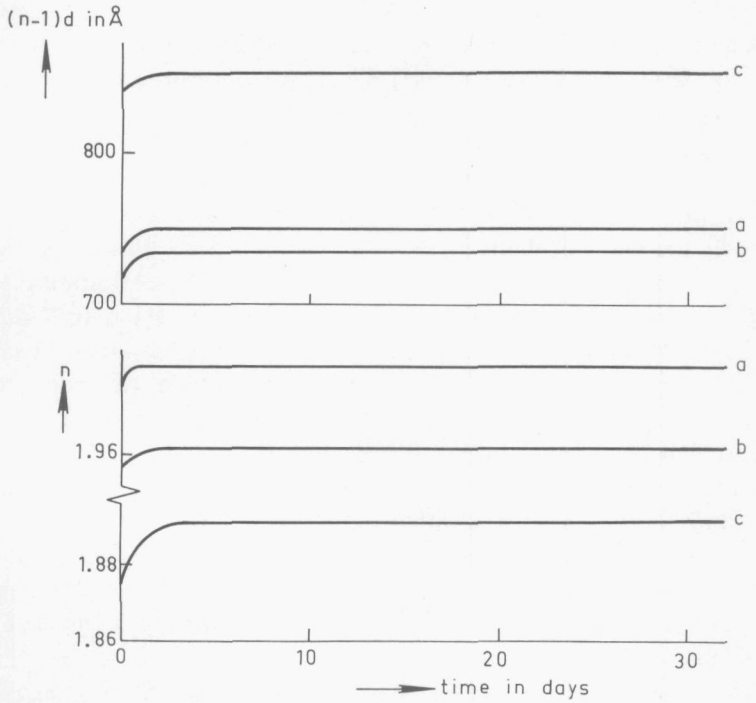

Fig. 36. Measured aging effects in the parameters $(n-1)d$ and n of cerium dioxyde films. The figure is a continuation of Table XI. Time zero corresponds with the first measurement in moist air.

after aging appears to depend strongly on the evaporation pressure and deposition rate. This is why it is difficult to obtain a good reproducebility, which can be seen from film a and b in table XI and fig. 36. By far the largest part of the changes in $(n-1)d$ and n takes place immediately after the admittance of air.

The thickness d as calculated from the measured values of $(n-1)d$ and n does not change by aging. So the change in $(n-1)d$ is mainly caused by a change in n.

7. *Silicon monoxide films*

In contrast with the different kinds of films discussed up to now, silicon monoxide films show some absorption in the visible range. As discussed in III.B and IV.A.3 we have to know the extinction index k to correct the phase retardation and the refractive index measurement.

For the determination of the extinction index k we applied both methods discussed in III.B: (a) straightforward computation of k from the measured reflectivities and transmissivity at normal incidence, (b) calculation of k from the maxima and minima for the reflectivity or transmissivity measured at normal incidence with the aid of the rather simple formulas, given by HALL and FERGUSON [41], valid if $k \cdot 2\pi d/\lambda < 0.05$. In particular the method suggested by HALL and FERGUSON is very convenient in our case, because the monitoring system (I.B) is based on the measurement of maxima and minima of the reflectivity and transmissivity.

The extinction index appeared to be $k = 0.02 \pm 0.005$ for $\lambda = 5461$ Å. However, the absorption increases for shorter wave-lengths: $k = 0.06 \pm 0.005$ for $\lambda = 4040$ Å. For wave-lengths larger than 6000 Å the extinction index k is below 0.01. The error is determined by the reproducebility of the evaporation process. Within the measuring error the extinction index appeared to be independent of the deposition rate for the range 2 to 10 Å/s and of evaporation pressures between 10^{-4} and 10^{-5} mm Hg.

From chapter III.B and the values determined for k it follows that the correction of the phase retardation measured can be ignored in this case. According to fig. 29, however, the measurement for the refractive index needs to be corrected. The values of the refractive index given below are corrected using $k = 0.02$.

The results of some measurements of the parameters $(n-1)d$ and n of silicon monoxide films, using substrates with a refractive index $n_s = 1.52$, are given in table XII; the changes measured in $(n-1)d$ and n immediately after the admittance of air are very small. From this table it can be seen that the refractive index has some tendency to decrease somewhat if dry air is admitted and to increase if moist air is admitted.

If the films are removed from the vacuum chamber, however, the aging effects can be considerable large. We measured $(n-1)d$ and n of the same film practically at the

TABLE XII

silicon monoxide films	evaporation-pressure in mm Hg	deposition rate in Å/s	$(n-1)d$ in Å			n		
			vacuum	dry air	moist air	vacuum	dry air	moist air
a	10^{-5}	3	661	651	650	1.706	1.700	1.704
b	10^{-4}	8	565	569	562	1.747	1.741	1.745
c	10^{-4}	4	570	575	568	1.690	1.682	1.689

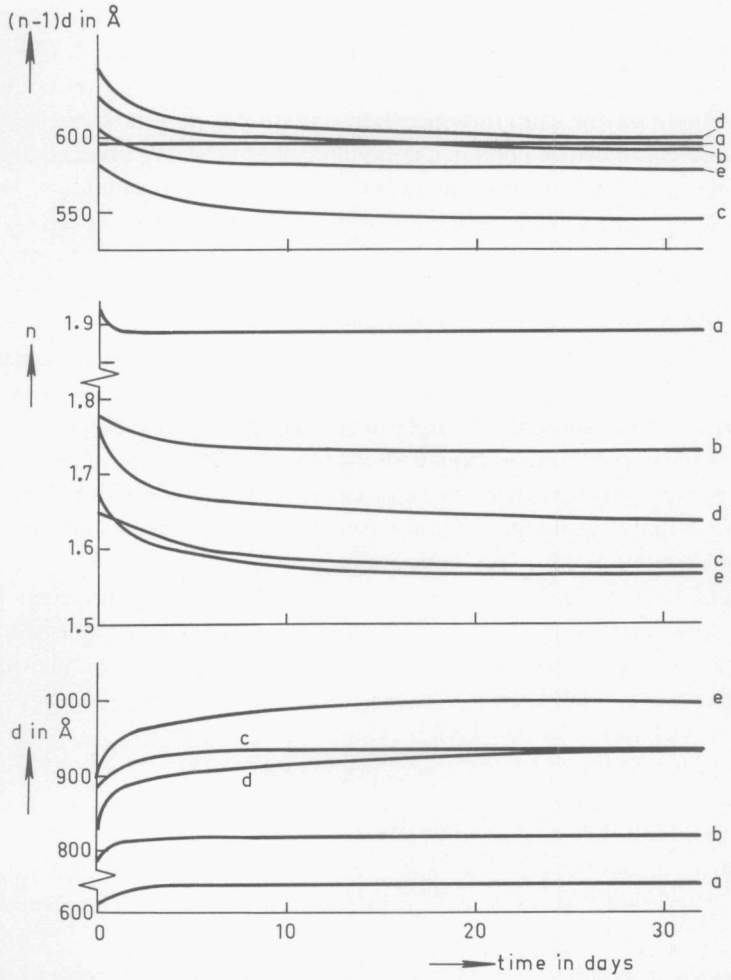

Fig. 37. Measured aging effects in the parameters $(n-1)d$ and n of silicon monoxyde films. Time zero corresponds with the moment that the films are removed from the vacuum chamber. The thickness d versus the time is calculated from the measured values of $(n-1)d$ and n.

	a	b	c	d	e
Pressure during the evaporation in mm Hg:	10^{-5}	10^{-5}	10^{-5}	10^{-4}	10^{-4}
Deposition rate in Å/s:	7.0	4.7	2.8	8.0	4.0

same time, so that the thickness d could be calculated. Fig. 37 shows results of measurements of $(n-1)d$ and n together with the calculated thickness d versus the time for different deposition rates and evaporation pressures. The deposition rate varied from 2 to 8 Å/s and the evaporation pressure was 10^{-4} or 10^{-5} mm Hg. Generally speaking fig. 37 shows that the changes in $(n-1)d$ and n as well as n itself depend very strongly on the deposition rate and evaporation pressure. The refractive index n

decreases stronger with time than the parameter $(n-1)d$, so that the thickness d increases with time. Only at a high deposition rate (7 Å/s) and a low evaporation pressure (10^{-5} mm Hg) are the aging effects small. Because the refractive index n depends strongly on the evaporation conditions (in our case it varies between 1.97 and 1.57) it is very difficult to obtain a good reproducebility. We attained a reproducebility within a few units in the second decimal of the refractive index.

8. *Multilayers*

Up to now we have discussed aging effects measured in the case of single dielectric films. However, it is of practical interest to know whether similar effects occur in multilayers, i.e. combinations of single dielectric films with different refractive indices. This is important in connection with the manufacture of anti-reflection coatings, interference filters, mirrors for lasers and beam splitters. The number of materials, which are used in different kinds of multilayers is very large. We will restrict ourselves to a multilayer often used in our optics department.

In the same way as described above we have measured the equivalent parameter $(n-1)d$ of some double layers. The materials are successively evaporated from two boats, so that it is not necessary to admit air into the vacuum chamber during the evaporation process. An example is given in table XIII.

TABLE XIII

evaporation pressure in mm Hg	deposition rate in Å/s	$(n-1)d$ in Å					
		thorium fluoride	thorium fluoride + zinc sulphide		zinc sulphide	zinc sulphide + thorium fluoride	
		vacuum	vacuum	moist air	vacuum	vacuum	moist air
10^{-5}	20	494	1280	1310	804	1271	1365

In both cases represented in table XIII the parameter $(n-1)d$ increases further by about 10 Å if the double layers are removed from the vacuum chamber. According to chapter V.B.5 it is reasonable to assume that these aging effects are caused mainly by thorium fluoride. The aging effect of the double layer in which the zinc sulphide is first evaporated agrees reasonably well with the aging of a comparable single film of thorium fluoride (see V.B.2). The aging effect of the double layer in which thorium fluoride is first evaporated is smaller. The aging effect of this thorium fluoride film is probably smaller, because this film is enclosed between the substrate and the zinc sulphide film.

According to our measurements interference filters built up from two highly reflecting multilayer (thorium fluoride and zinc sulphide) mirrors separated by a single thorium fluoride film appeared to show practically no aging effect after removal from the vacuum chamber.

C. Conclusion

The purpose of the measurements was to obtain quantitative data (V.B) of aging of dielectric films, a phenomenon which was qualitatively observed earlier [45]. From the data obtained it appears that the aging effects differ considerably for the various film materials commonly used. Moreover the results have confirmed the necessity of the measurements in vacuo, because for a number of materials the largest part of the changes in the parameters $(n-1)d$ and n takes place immediately after the admittance of air into the vacuum chamber.

Although we have not investigated the mechanism of the aging effects, we nevertheless wish to point out that the measurements strongly suggest that a part of the aging of the fluorides, zinc sulphide and cerium dioxide is caused by adsorption of air and water. The decrease in the refractive index of silicon monoxide films is probably caused by oxidation of the film.

Once more we wish to stress the necessity of specifying the experimental conditions when studying aging effects; it is quite possible that under different conditions entirely different results would be obtained. We mention a discrepancy between our refractive index measurements and those known from literature. HOLLAND [46] for instance gives for the refractive index of cerium dioxide films $n = 2.2$, whereas after aging we find values between 1.85 and 2.00. An explanation for this effect could be a difference in purity content.

Although the aging effects certainly will play a role in the choice of the film material for practical purposes, the primary considerations determining this choice will concern characteristics like the refractive index, stress, durability, scattering, dispersion, etc.

Concerning the Abelès method we remark that this method can be improved by using photoelectric detection [44] in particular this is convenient if many refractive index measurements have to be carried out.

SAMENVATTING

Het doel van dit werk was kwantitatieve gegevens te verkrijgen betreffende veroudereringseffecten in de optische eigenschappen van diëlektrische dunne lagen. De karakteristieke optische parameters van deze lagen zijn de optische dikte, de brekingsindex en de eventuele absorptie. Om de veranderingen in de optische parameters te kunnen bestuderen, is het nodig over middelen te beschikken om de parameters in vacuo onmiddellijk na het opdampen te kunnen meten. In de inleiding wordt daarom een kort overzicht gegeven van de bestaande methoden voor het meten van optische parameters van dunne films. Alleen methoden die direct de gevraagde parameters geven, komen in aanmerking. Bovendien moest ook in vacuo gemeten kunnen worden, waarbij de gevoeligheid tamelijk hoog moest zijn. Er bestaan enige interferometrische meetmethoden, zoals die van VAN HEEL en WALTHER en de driespletenmethode van ZERNIKE, die gemakkelijk in het gebruik zijn. Zulke interferometrische metingen met het substraat in transmissie hebben het voordeel gemeen dat een faseverschil gemeten wordt, waaruit op eenvoudige wijze de optische parameter $(n-1)d$ kan worden afgeleid. Teneinde de fout in de meting van het optisch weglengteverschil binnen $\lambda/1000$ te houden, was het nodig een fotoëlektrisch instelkenmerk te gebruiken in plaats van een direct visueel instelkenmerk. Een extra voordeel van fotoelektrische interferometers is dat slechts een geringe lichtintensiteit nodig is. Daardoor was het mogelijk een zeer eenvoudig interferometer type te gebruiken, gebaseerd op de tweespletenproef van YOUNG.

Deze interferometer wordt beschreven in hoofdstuk II. De fasevertraging door de laag wordt bepaald door meting van de verschuiving van het interferentiepatroon, die optreedt als de laag voor een van de twee spleten wordt geplaatst. Eerst wordt een opstelling beschreven, waarin een visueel instelcriterium volgens FRANÇON en SOULIÉ wordt gebruikt. In feite is dit een fotometrische methode, waarbij wordt ingesteld op een minimum in het buigingspatroon; het criterium is dan de symmetrie van de waargenomen intensiteitsverdeling. Verder worden drie fotoëlektrische interferometers beschreven: (a) een opstelling, waarin het licht door het preparaat gaat, (b) een opstelling, waarin het licht aan het preparaat wordt gereflecteerd en (c) een opstelling voor metingen in vacuo. Teneinde een fotoëlektrisch instelkenmerk te verkrijgen, wordt het interferentiepatroon tijdharmonisch in positie gemoduleerd. De modulatie wordt verkregen door een roterende scheefstaande planparallelle glasplaat. De positie van de interferentiestrepen wordt gedetecteerd met behulp van een spleet en een fotomultiplier. Het fotoëlektrische signaal is een cosinus-functie, waarvan de fase is samengesteld uit de volgende drie bijdragen: (a) de positie van de spleet, (b) het fase-

verschil tussen de interfererende bundels en (c) een term voor de tijdharmonische modulatie. In het fourierspectrum verdwijnen de oneven harmonischen, in het bijzonder dus de grondharmonische, als de twee eerstgenoemde bijdragen nul zijn. Het instelkenmerk voor deze situatie is de visuele waarneming van de onvervormde tweede harmonische op een oscilloscoopscherm. De theorie van deze interferometers wordt gegeven, waarbij rekening wordt gehouden met de coherentiegraad, de eindige spleetbreedte van de dubbele spleet en het verschil in intensiteit tussen de twee interfererende bundels.

Het gemeten faseverschil van de laag is gelijk aan $2\pi(n-1)d/\lambda$, indien de multipele reflecties en de absorptie kunnen worden verwaarloosd. In hoofdstuk III wordt de geldigheid van deze benadering besproken in verband met de hoge nauwkeurigheid van de metingen.

Voor de directe meting van de brekingsindex van een dunne diëlektrische laag hebben we de methode van ABELÈS gekozen, vanwege de nauwkeurigheid en eenvoud. De methode berust erop, dat indien een substraat gedeeltelijk is voorzien van een volledig transparante laag, de intensiteit van de reflectie aan het bedekte en die aan het onbedekte deel van het substraat aan elkaar gelijk zijn, indien de hoek van inval gelijk is aan de Brewsterhoek van de laag. Dit geeft een zeer eenvoudige methode om de brekingsindex van volledig transparante, homogene, isotrope dunne lagen te meten. In hoofdstuk IV wordt de gevoeligheid van deze methode besproken. Er wordt een beschrijving gegeven van een opstelling voor metingen in lucht en een opstelling voor metingen in vacuo. In het tweede geval moesten speciale maatregelen genomen worden om hoekmetingen in de vacuümklok te vermijden.

In hoofdstuk V worden enige meetresultaten gegeven betreffende de veranderingen in de optische parameters $(n-1)d$ en n van diëlektrische dunne lagen ten gevolge van veroudering. Hierbij hebben we ons beperkt tot die stoffen die vaak gebruikt worden in de optische praktijk. De lagen worden vervaardigd door opdampen van de betreffende stof in een vacuümklok. Er zijn metingen gedaan bij verschillende opdampsnelheden en opdampdrukken. Uit de verkregen gegevens blijkt dat de verouderingseffecten van de verschillende stoffen aanzienlijk uiteenlopen. Verder blijkt dat het verouderingsproces in twee stappen gebeurt: (a) een vrijwel momentane verandering na het toelaten van lucht en (b) een meer geleidelijke verandering in de loop van enkele dagen.

REFERENCES

1. S. METHFESSEL — Dünne Schichten, VEB Wilh. Knapp Verlag, Halle 1953
2. G. C. MÖNCH — Optik **9** (1952) 75
3. C. DUFOUR — Vide **3** (1948) 480
4. C. DUFOUR — J. Phys. Radium **11** (1950) 353
5. C. FRÉMONT — Rev. Sci. Instr. **20** (1949) 620
6. W. STECKELMACHER, J. M. PARISOT, L. HOLLAND and T. PUTNER — Vacuüm **9** (1959) 171
7. P. GIACOMO and P. JACQUINOT — J. Phys. Radium **13** (1952) 59A
8. F. ABELÈS — J. Phys. Radium **11** (1950) 310, 403
9. F. ABELÈS — J. Phys. Radium **19** (1958) 327
10. P. DRUDE — Ann. Phys. Chem. **39** (1890) 481
11. A. HERMANSEN — Nature **167** (1951) 104
12. M. FRANÇON — Rev. d'Opt. **31** (1952) 65
13. A. C. S. VAN HEEL and A. WALTHER — Opt. Act. **5** (1958) 47
14. F. DYSON — Physica **24** (1958) 532
15. S. TOLANSKY — Multiple Beam Interferometry, University Press, Oxford 1948
16. K. M. GREENLAND and C. BILLINGTON — J. Phys. Radium **11** (1950) 418
17. L. G. SCHULZ — J.O.S.A. **40** (1950) 690
18. P. D. FOCHS — J.O.S.A. **40** (1950) 623
19. R. PRAT and M. L. ROBLIN — Rev. d'Opt. **45** (1966) 3
20. F. ZERNIKE — J.O.S.A. **40** (1950) 326
21. Y. VÄISÄLÄ — Thesis, Helsinki 1922
22. A. C. S. VAN HEEL — Physica **24** (1958) 529
23. A. LOHMANN — Zst Phys. **143** (1956) 533
24. F. Z. KEISTER and R. Y. SCAPPLE — Ninth National Symposium on Vacuum Technology Transactions 1962, page 116, McMillan, New York 1962
25. K. H. BEHRNDT — Z. Angew. Phys. **8** (1956) 453
26. K. H. BEHRNDT — Physics of thin films III, edited by G. Hass and R. E. Thun, page 21, New York 1966
27. P. LOSTIS — Rev. d'Opt. **38** (1959) 1
28. A. WOOD — Thomas Young (natural philosopher) page 176, University Press, Cambridge 1954
29. M. FRANÇON and Miss A. SOULIÉ — Rev. d'Opt. **42** (1963) 499
30. K. M. BAIRD — J.O.S.A. **44** (1954) 11
31. R. D. HUNTOON, A. WEISS and W. SMITH — J.O.S.A. **44** (1954) 264
32. R. J. KENNEDY — Proc. Nat. Acad. Sci. Wash. **12** (1926) 621
33. M. BOTTEMA — Photometric setting methods in interferometry, thesis, Groningen 1957
34. E. T. WHITTAKER and G. N. WATSON — A course of modern analysis, page 379, Cambridge 1962
35. M. BORN and E. WOLF — Principles of Optics, page 505, Oxford 1965
36. M. BORN and E. WOLF — Principles of Optics, page 510, Oxford 1965
37. H. MAYER — Physik dünner Schichten I (1950) and II (1955) Stuttgart

38. O. S. Heavens — Optical properties of thin solid films, London 1955
39. A. Vašiček — Optics of thin films, Amsterdam 1960
40. M. Born and E. Wolf — Principles of Optics, page 627, Oxford 1965
41. J. F. Hall and W. F. C. Ferguson — J.O.S.A. **45** (1955) 714
42. A. C. Traub and H. Osterberg — J.O.S.A. **47** (1957) 62
43. J. F. Hall and W. F. C. Ferguson — J.O.S.A. **45** (1955) 74
44. J. T. Cox and G. Hass — Physics of thin films II, edited by G. Hass and R. E. Thun, page 272, New York 1964
45. O. S. Heavens and S. D. Smith — J.O.S.A. **47** (1957) 469
46. L. Holland — Vacuum deposition of thin films, page 513, London 1956
47. O. S. Heavens — Physics of thin films II, edited by G. Hass and R. E. Thun, page 212, New York 1964.

STELLINGEN

I

Het is mogelijk een indruk te verkrijgen over de uniformiteit van de laagdikte bij het opdampen van diëlektrische lagen door zo'n laag als tussenlaag van een interferentiefilter te gebruiken en dan van dit filter de golflengte, waarbij de transmissie maximaal is, te bepalen als functie van de plaats op het filter.

II

Ten onrechte suggereren COX en HASS dat een antireflectiecoating bestaande uit vier $\frac{1}{4}\lambda$-lagen niet vervaardigd kan worden voor het zichtbare gebied.

J. T. COX en G. HASS, Physics of thin films II, edited by G. Hass and R. E. Thun, page 273, New York 1964.

III

De bewering van HEAVENS betreffende de invloed van absorptie op het meten van de brekingsindex van zwak absorberende lagen met de methode van Abelès is onjuist.

O. S. HEAVENS, Physics of thin films II, edited by G. Hass and R. E. Thun, page 211, New York 1964.

IV

De in dit proefschrift beschreven methode van Abelès is bijzonder geschikt als practicumproef voor studenten in de natuurkunde.

V

Om het opdampproces te volgen, wordt in de praktijk veelal gebruik gemaakt van de gemakkelijke maar principieel onnauwkeurige methode, waarbij wordt ingesteld op een extremum van de reflectie of transmissie. Er is dringend behoefte aan een praktisch bruikbare, nauwkeurige methode.

VI

Het is mogelijk dunne lagen met een voorgeschreven brekingsindex te vervaardigen door uit meerdere bronnen tegelijkertijd verschillende stoffen op te dampen. Het verdient aanbeveling deze methode verder te ontwikkelen.

VII

Het gebruik van de uitdrukking „koude straling", veel gebezigd in de warmtetechniek, werkt misverstand in de hand.

VIII

Het moet betwijfeld worden of het voordeel van brilleglazen met een continu verlopende sterkte opweegt tegen de nadelen. Dat van niet-medische zijde deze glazen worden aangeprezen is ongewenst.

IX

Ten onrechte wordt door KINZLY de interferometer met drie spleten als nieuw geïntroduceerd.

Y. VÄISÄLÄ, dissertatie, Helsinki 1922.
F. ZERNIKE, J.O.S.A. **40** (1950) 326.
R. E. KINZLY, Applied Optics **6** (1967) 137.

X

Bij de verlichting van kruispunten, overwegen enz. is het wenselijk grote discontinuïteiten te vermijden.

W. van Vonno
8 mei 1968